



Matzke-Ogi, A. et al. (2016) Inhibition of tumor growth and metastasis in pancreatic cancer models by interference with CD44v6 signaling. *Gastroenterology*, 150(2), 513-525.e10. (doi:10.1053/j.gastro.2015.10.020)
This is the author's final accepted version.

There may be differences between this version and the published version.
You are advised to consult the publisher's version if you wish to cite from it.

<http://eprints.gla.ac.uk/116680/>

Deposited on: 25 April 2016

Efficient Treatment of Metastatic Pancreatic Cancer via Targeted Inhibition of CD44v6 Signaling

Alexandra Matzke-Ogi^{1,2}, Katharina Jannasch^{3§}, Marine Shatirishvili^{§1}, Beatrix Fuchs^{§1}, Sara Chiblak^{5,6}, Jennifer P Morton⁸, Bouchra Tawk^{5,6}, Thomas Lindner⁹, Owen J Sansom⁸, Frauke Alves³, Arne Warth⁴, Christian Schwager^{5,6}, Walter Mier⁹, Jörg Kleeff⁷, Helmut Ponta², Amir Abdollahi^{5,6} and Véronique Orian-Rousseau^{1*}

¹ Karlsruhe Institute of Technology, Institute of Toxicology and Genetics, Hermann-von-Helmholtz Platz 1, 76344 Eggenstein-Leopoldshafen, Karlsruhe, Germany

² amcure GmbH, Hermann-von-Helmholtz Platz 1, 76344 Eggenstein-Leopoldshafen

³ Department of Hematology and Oncology, University Medicine Göttingen, Robert-Koch-Str. 40, 37075 Göttingen, Germany

⁴ Institute of Pathology, University Hospital Heidelberg, Heidelberg, Germany

⁵ Molecular and Translational Radiation Oncology, Heidelberg Institute of Radiation Oncology (HIRO), University of Heidelberg Medical School and German Cancer Research Center (DKFZ), Im Neuenheimer Feld 450, 69120, Heidelberg, Germany

⁶ The German Cancer Consortium (DKTK), Heidelberg, Germany

⁷ Department of Surgery, Technische Universität München, Ismaningerstr. 22, 81675 Munich, Germany

⁸ Cancer Research UK Beatson Institute, Garscube Estate, Switchback Road, Glasgow G61 1BD, United Kingdom

⁹ Department of Nuclear Medicine, University of Heidelberg, Im Neuenheimer Feld 400, Heidelberg, Germany

[§]these authors contributed to the same extent to the paper

*corresponding author

Karlsruhe Institute of Technology, Institute of Toxicology and Genetics, Karlsruhe, Campus North, Postfach 3640, 76021 Karlsruhe, Germany

Email: veronique.orian-rousseau@kit.edu

Phone: 0049 721-608-26523

Fax: 0049 721-608-23354

Running title: CD44v6 peptides eliminate pancreatic metastases

Alexandra Matzke-Ogi: generation, analysis and interpretation of the data

Katharina Jannasch: generation, analysis and interpretation of part of the data

Marine Shatirishvili: generation, analysis and interpretation of part of the data

Beatrix Fuchs: generation, analysis and interpretation of part of the data

Sara Chiblak: generation, analysis and interpretation of part of the data

Jennifer Morton: generation, analysis and interpretation of part of the data

Bouchra Tawk: generation, analysis and interpretation of part of the data

Thomas Lindner: generation, analysis and interpretation of part of the data

Owen Sansom: analysis and interpretation of part of the data

Frauke Alves: designed part of the study, analyzed and interpreted part of the data

Arne Warth: generation, analysis and interpretation of part of the data

Christian Schwager: generation, analysis and interpretation of part of the data

Walter Mier: analysis and interpretation of part of the data

Jörg Kleeff: collection and assembly of part of data

Helmut Ponta: analysis, interpretation of the data, participated in the conception of the data and in the writing of the manuscript

Amir Abdollahi: analysis, interpretation of the data, participated in the conception of the data and in the writing of the manuscript

Véronique Orian-Rousseau: analysis, interpretation of the data, conception and design of the data, wrote the manuscript

Conflict of interest

Alexandra Matzke-Ogi (AMO), Helmut Ponta (HP) and Véronique Orian-Rousseau (VOR) are co-founders and share holders of the start-up company amcure GmbH which develops a CD44v6 targeting peptide for clinical study. For this reason AMO, HP and VOR have a conflict of interest.

AMO, HP are currently employees of amcure. No financial support was provided by amcure for the studies which are topic of this manuscript. Amcure does not develop the peptides presented in this study for clinical tests but modifications thereof.

This work presented here was supported by grants of the Deutsche Forschungsgemeinschaft (OR 124/4-1 and 2) and was not part of an industrial

development.

Katharina Jannasch, Marine Shatirishvili, Beatrix Fuchs, Sara Chiblak, Jennifer Morton, Bouchra Tawk, Thomas Lindner, Owen Sansom, Frauke Alves, Arne Warth, Christian Schwager, Walter Mier, Jörg Kleeff and Amir Abdollahi have no conflict of interest.

Patent EP1647556: composition of matter - CD44v6 peptides

Abstract

Background and Aims: Cancer cells with high metastatic potential and stem cell like characteristics express the cell surface marker CD44. However, the molecular mechanism of action of CD44 in tumor progression and metastasis remains elusive. We sought to explore the impact of CD44v6 signaling in pancreatic cancer growth and metastasis.

Methods: Tumor cells expressing different CD44 isoforms including CD44v6 and v6 peptides interfering with the CD44v6 co-receptor function for Met and VEGFR-2 were tested in syngeneic rat (ASv6), orthotopic murine (FC1245-KPC) and human (L3.6pl, Panc1) as well as patient derived tumor xenografts (PDTX, JoPaca-1). The CD44v6 peptide was further tested in the KPC (*LSL-Kras*^{G12D/+}, *LSL-Trp53*^{R172H/+}, *Pdx1-Cre*) genetically engineered mouse (GEM) model. The expression of CD44v6 transcripts was interrogated in RNA-sequencing data from 136 pancreatic cancer patients.

Results: CD44v6 was found to be a prerequisite for pancreatic cancer metastasis. The pro-metastatic effect of CD44v6 was reversed by Met knockdown. Inhibitory CD44v6 peptides reduced the metastatic tumor burden in all models. Intriguingly, regression of already established metastatic lesions was observed after CD44v6 blockade. Elevated tumor CD44v6 expression was associated with enhanced Met expression and correlated with poor patient survival and increased metastasis. CD44v6 inhibition correlated with reduced Met-dependent cell migration/invasion, enhanced ligand-induced apoptosis and reduced VEGFR-2-dependent angiogenesis. Of note, CD44v6 inhibition more efficiently prevented metastasis compared to mono/dual Met (Crizotinib) and VEGFR-2 (Pazopanib) inhibition.

Conclusion: Therefore, CD44v6 organizes a signaling hub for pancreatic cancer metastasis hence providing an attractive novel therapeutic target for this devastating disease.

Introduction

Metastatic tumor growth remains the major reason for cancer treatment failure.¹ Early distant dissemination is a characteristic feature of the most aggressive types of cancers, among which is pancreatic cancer, leading to poor prognosis. Metastatic cells have acquired specific properties distinguishing them from the locally growing tumor cells. These features are determined by key proteins controlling cell behavior and cell fate. One such protein is CD44, a family of transmembrane glycoproteins involved in many cellular processes including proliferation, migration, and survival (reviewed by Orian-Rousseau²). Family members differ in the extracellular domain where 10 variant exons are either excluded or included in various combinations. There is ample evidence for increased expression of CD44 isoforms in tumor progression and metastasis (reviewed by Zoller³). In addition, CD44 is present on several types of cancer stem cells. Previous approaches aimed at targeting these cellular subpopulations, for example, via delivery of toxins with limited preclinical and clinical success (reviewed by Orian-Rousseau and Ponta⁴).

CD44v6, a CD44 family member, is critical for signaling as a co-receptor for receptor tyrosine kinases (RTKs) such as MET, recepteur d'origine nantais (Ron), and vascular endothelial growth factor receptor-2 (VEGFR-2) (reviewed by Orian-Rousseau²). MET is involved in biological processes such as migration, invasion, proliferation, survival, and epithelial remodeling, crucial steps for dissemination of tumor cells.⁵ Overexpression, mutations, or mis-expression of MET or its ligand hepatocyte growth factor (HGF)/scatter factor has been observed in a wide range of cancers.⁶ The cooperation between CD44v6 and MET involves both the ectodomain of CD44v6 as well as the cytoplasmic domain. In several cancer cell lines as well as in primary cells, HGF-induced MET phosphorylation depends on CD44v6.⁷ Scanning mutations in the exon v6 located in the CD44v6 ectodomain showed the importance of 3 amino acids in the center of this exon.⁸ These amino acids are RWH in human, GWQ in mouse, and EWQ in rat. Peptides covering these 3 amino acids block MET activation in many different cell systems.^{8 and 9} CD44v6 also collaborates with VEGFR-2, which plays a critical role in angiogenesis.¹⁰ The CD44v6 peptides also can block VEGF-induced VEGFR-2 activation and signaling.⁹

Together, these data add to the relevance of CD44v6 signaling in tumor growth and metastasis. Therefore, we aimed to investigate the impact of CD44v6 in pancreatic cancer metastasis. Here, we show that this co-receptor function of CD44v6 for MET is the driving force for metastasis in several independent pancreatic cancer models. Furthermore, small peptides interfering with CD44v6⁸ block metastatic spreading

and, most importantly, lead to regression of already established metastases. These effects of the CD44v6 peptide, especially on distant metastases, suggest a potential for treatment of pancreatic cancer, a fast metastasizing cancer.

Results

Both CD44v6 and MET Control Metastatic Spreading of Rat Pancreatic Tumor Cells

Only CD44 isoforms containing exon v6 sequences with any combination with other variant exons, including CD44v6,7, CD44v4-7, or CD44v1-10, can act as co-receptors for the RTK MET.⁷ In the rat pancreatic carcinoma BSp73AS cells expressing only CD44s, MET cannot be activated by HGF unless a CD44v6-containing isoform is expressed (Figure 1A), in line with previous observations.⁷ Moreover, exon v6 removal in CD44v1-10Δv6 impaired MET activation (Figure 1A). To test whether the CD44v6 co-receptor function for MET would be necessary for induction of the metastatic potential in nonmetastatic BSp73AS cells, BSp73AS cells expressing different CD44 isoforms were injected subcutaneously into syngeneic rats. In all cases, a primary tumor was detected (Supplementary Table 1). Strikingly, only in the case of ASv6 (designated CD44v6) and ASv1-10 (designated CD44v1-v10) cells were metastases detected in the axillary lymph nodes at the injection site (Figure 1B and Supplementary Table 1). No pulmonary metastases were detected in animals injected with parental cells or cells transfected with CD44v1-10Δv6 (Figure 1B and Supplementary Table 1), whereas CD44v6 and CD44v1-v10–transfected cells efficiently colonized the lungs. We then tested whether MET inactivation also prevented metastasis. Importantly, the metastatic potential conferred by the CD44v6 isoforms was MET-dependent, as shown by knock-down experiments. ASv6 cells infected with lentivirus-expressing MET shRNA sequences¹⁴ (Figure 1A, last 2 lanes) were injected (or cells expressing control shRNA sequences) subcutaneously into rats. All animals developed primary tumors even upon knock-down of MET. However metastasis was abrogated (Figure 1B and Supplementary Table 1). MET activation was observed only in primary tumors expressing control shRNA, but not MET shRNA (Figure 1C).

Our experiments showed that CD44v6 and MET are required together for metastatic spreading of CD44v6-transfected AS cells.

CD44v6 Peptides Inhibit Metastasis of Rat Pancreatic Tumor Cells

We identified 3 species-specific amino acids encoded by exon v6 that are relevant for the CD44v6 co-receptor function.⁸ Peptides of 5-14 amino acids length containing the 3 crucial amino acids inhibit HGF-induced MET and downstream Erk activation as efficiently as a CD44v6 blocking antibody (Figure 2A), in line with our previous observations.⁸ In addition, the PI3K/Akt pathway was impaired as detected by phospho-AKT Western blot (Figure 2A). We examined whether this interfering peptide also would inhibit CD44v6-dependent metastasis. ASv6 cells were injected subcutaneously into syngeneic rats and 1 week later the rat CD44v6 peptide (designated rv6pep), a control peptide, or the CD44v6 blocking antibody was injected intratumorally (Supplementary Figure 2) or intravenously (Figure 2B–D) 3 times a week for 3 weeks. Treatment with the v6 blocking antibody or with rv6pep had no effect on primary tumor growth (Figure 2B and Supplementary Table 2). Importantly, metastasis was completely inhibited by rv6pep and the CD44v6 monoclonal antibody (Figure 2C and D, Supplementary Table 2, and shown for BSp73AS cells expressing CD44v4-7¹⁵).

The specificity of the CD44v6 peptides binding to the tumor and to the metastases in vivo was shown using DY681-labeled peptide in near-infrared fluorescence imaging with the Optix MX2 (ART, Montreal, Canada) (Supplementary Figure 3).

Taken together, our experiments strongly suggest that the CD44v6 co-receptor function for MET is a crucial step for metastatic spreading in the rat syngeneic pancreatic tumor model and that CD44v6 peptides not only inhibit metastasis formation but also specifically target local and metastatic tumor cells in vivo.

In an Orthotopic Syngeneic Murine Pancreatic Model a CD44v6 Peptide Decreases Tumorigenesis and Prevents Metastasis

The KPC (LSL-Kras^{G12D/+}, LSL-Trp53^{R172H/+}, Pdx1-Cre) mice carrying a pancreatic-specific Trp53^{R172H} mutation alongside an initiating mutation in Kras^{G12D} recapitulate the pathophysiological and molecular features of human pancreatic ductal adenocarcinoma (PDAC).¹⁶ These mice develop invasive metastatic PDAC with an extensive stroma and, in common with human PDAC, are insensitive to therapy.

13 and 17

FC1245 cells are pancreatic carcinoma cells derived from these KPC mice. In these cells MET activation could be inhibited by treatment with mv6pep and with the

MET kinase inhibitor crizotinib, approved for lung cancer,¹⁸ but not with rv6pep (control peptide) (Figure 3A). Furthermore, the HGF-dependent migration of these cells, as monitored by a scratch assay, was blocked in a concentration-dependent fashion by mv6pep and crizotinib (Supplementary Figure 4). Orthotopic transplantation of FC1245 cells into syngeneic mice gave rise to pancreatic carcinoma with metastases in liver, spleen, and kidney (Supplementary Table 3). Upon treatment of the animals with crizotinib, both tumor growth and metastasis were inhibited (Figure 3B and C). Most importantly, mv6pep treatment also reduced primary tumor growth and metastasis. This effect was even stronger than that observed with crizotinib (Figure 3B and C and Supplementary Table 3). MET activation in the tumors using phospho-MET staining as readout was completely inhibited by mv6pep treatment, but only partially inhibited by crizotinib (Figure 3D).

Direct treatment of KPC mice with mv6pep after they already had developed clinically detectable palpable pancreatic tumors and metastases¹⁹ resulted in a dramatic prolongation of their life span (Figure 3E).

Growth of Primary Tumor and Metastasis of Human Pancreatic Cancer Cells Is Inhibited by a Human CD44v6 Peptide

To expand our studies to human pancreatic tumors we made use of the highly metastatic human pancreatic carcinoma cells L3.6pl¹¹ and the highly tumorigenic primary human pancreatic tumor cells JoPaca-1, characterized by a high expression of cancer stem cell markers and a high clonogenic potential in vitro and in vivo.²⁰ In both systems MET activation is CD44v6-dependent (Figure 4A) (as reviewed by Tremmel et al.⁹). We orthotopically injected these cells into immune-compromised mice. These mice developed primary tumors after 1 week, and numerous metastases after 3–4 weeks with L3.6pl and 10 weeks with JoPaca-1 cells (Supplementary Tables 4 and 5). The primary tumors expressed large amounts of CD44v6 (Figure 4C). Of note, the body weight of animals in the JoPaca-1 Patient Derived Tumor Xenograft (PDX) model did not significantly change after peptide treatment for a long time period (eg, 80 days) (Figure 4B).

MET was activated in the tumor sections as shown in the case of the L3.6pl cells (Supplementary Figure 6A). Intraperitoneal injection of hv6pep 3 times per week for 3 weeks completely repressed MET activation (Supplementary Figure 6A), showing interference of the peptide with the CD44v6 co-receptor function for MET. Because MET activation is species-specific and the human MET receptor can be activated

only by human HGF,²¹ this result suggests that L3.6pl cells produce their own HGF. Indeed, human HGF at a concentration of 1470 pg/mL was detected in the L3.6pl supernatants after 5 days of culture (Supplementary Figure 6B). Interestingly, the v6 peptide repressed this HGF secretion (Supplementary Figure 6B).

The outgrowth of the orthotopic human (L3.6pl and JoPaca-1) (Figure 4C) and murine (FC1245) (Figure 3B) tumors was strongly repressed by hv6pep and mv6pep, respectively. This is in contrast to the subcutaneously growing rat model (Figure 2B). One explanation is that the local growth of the rat model is primarily independent of CD44v6 and MET (Figure 2B and Supplementary Table 1). Hence, the tumor originally was selected to survive the artificial subcutaneous microenvironment, and introduction of CD44v6 expression confers only a prometastatic effect that could be abrogated by the v6 peptide. Furthermore, treatment with hv6pep decreased angiogenesis in the L3.6pl orthotopic model (Supplementary Figure 6C) similar to our observation with mv6pep.⁹ Because the v6 peptides are species-specific, angiogenesis inhibition by hv6pep cannot be the result of an effect on the murine endothelial cells in the xenograft systems but rather of an inhibition of VEGF production by the human cells. Indeed, L3.6pl cells produce hVEGF, a secretion that can be blocked with the hv6pep (Supplementary Figure 6B). Of note, VEGFR-2 activation *in vivo* was reduced by hv6pep treatment (Supplementary Figure 6A).

The most striking observation with the human pancreatic tumor models was the strong inhibition of metastasis by hv6pep (Figure 4D and Supplementary Tables 4 and 5) as compared with the rat-specific control peptide.

Finally, our findings were recapitulated with another model, namely the orthotopic injection of Panc1 cells²² in immune-compromised mice (Supplementary Figure 7 and Supplementary Table 6).

Because the CD44v6 peptide inhibits primary tumor growth and metastasis of human pancreatic cancer cells in the tested tumor models, the CD44 co-receptor function for MET and VEGFR-2 might be involved in human pancreatic cancer. We examined CD44v6, MET, and VEGFR-2 expression using RNA-seq data of human pancreatic cancer patients (Figure 4E and Supplementary material). The patient cohort was divided into 2 clusters according to tumor CD44v6 high (up) vs CD44v6 low (down) expression. In the CD44v6 up group patients had a significantly increased odds ratio of metastasis of 44%, vs 23% of patients in the v6 down group ($P = .01$). Furthermore, patients in the v6 up group had a significant (~4-fold) increase in

median expression of MET (Figure 4E) ($P = .01$, adjusted Bonferroni). There was no significant difference in the mean expression of VEGFR-2. Patients with high tumor expression of v6-containing transcripts had a significantly shorter median survival of approximately 13 months compared with patients with low tumor v6 expression (median survival, 18 mo; $P = .02$; log-rank) (Figure 4F).

Because the CD44v6 peptide also interferes with MET⁸ and VEGFR-2 function,⁹ we then tested whether inhibition of both RTKs with a combination of inhibitors would have a similar effect as the peptide alone. To this aim, we compared the efficacy of hv6pep on primary tumor growth and metastasis with treatment with crizotinib or pazopanib. Of note, both inhibitors already are approved for the treatment of human cancers.^{18 and 23} Crizotinib has been described previously. Pazopanib targets several RTKs, including VEGFR-2. Both inhibitors repressed primary tumor outgrowth, particularly when used together, similar to the treatment with hv6pep (Figure 5A). In addition, liver metastasis was hampered by both inhibitors, again most effective when used in combination (Figure 5B and C). However, this repression was much less effective than treatment with hv6pep (Figure 5B and C).

Already Established Metastases Are Eliminated by CD44v6 Peptides

To decisively explore whether the CD44v6 peptides can be used in a therapeutic setting on already established metastases, we injected ASv6 cells subcutaneously into syngeneic rats and L3.6pl cells orthotopically into nude mice and let them grow for 3 weeks, when all animals from the control groups had developed metastases (Supplementary Table 6). The animals then were treated either with the species-specific CD44v6 peptides or with control peptides 3 times per week for another 3 weeks (Figure 6A and B), and then were screened for metastases. As expected, metastases could be detected in all animals treated with the control peptides (Supplementary Table 6 and Figure 6A and B), whereas nearly all animals treated with the species-specific CD44v6 peptides were metastasis-free. Thus, already established metastases can be eliminated by treatment with the CD44v6 peptides. We next examined the lung for apoptosis using cleaved caspase-3 or caspase-8 as a read-out. Apoptotic cells were detected as early as 3 days after the first peptide injection in tumor areas of animals treated with rv6pep, but not with the control peptide (Figure 7). Maximum apoptosis was measured 8 days after the first peptide injection. At day 22, no metastases could be detected anymore in rv6pep-treated animals (Figure 7).

We then tested the efficiency of the peptide treatment in prolonging the survival of the animals. One week after injection of L3.6pl cells (when the animals already developed tumors as detected in the control group) (Figure 6C), animals were treated with hv6pep for 35 days. At that time (42 days), the tumors of the treated animals were reduced drastically but all control animals were moribund. Treatment then was stopped and the animals were observed for an additional 45 days. None of the remaining animals was moribund, but the primary tumor size did increase slightly, indicating tumor recurrence (Figure 6C). At autopsy, no macrometastases were observed in these animals.

Discussion

Here we show the critical relevance of CD44v6-dependent signaling in metastatic outgrowth of pancreatic tumor cells in human, rat and murine models. From the therapy perspective, we report intriguing inhibition of tumor growth and metastasis via blockade of CD44v6 signaling in a large series of orthotopic pancreatic cancer i.e., in well-characterized therapy refractory KPC-GEM and JoPaca-1 PDX models. This effect was in part via activation of at least two key metastasis-associated pathways, Met and VEGFR-2, respectively. Consequently, CD44v6 neutralizing peptides blocked Met and VEGFR-2 activation and abrogated the metastatic spreading of pancreatic tumor cells. Moreover, inhibition of CD44v6 signaling showed superior efficacy in orthotopic models over single or combined Met and VEGFR-2 RTK inhibitors currently used in the clinic. Hence CD44v6 signaling might control additional metastatic circuitries beyond its co-receptor function for Met and VEGFR-2. Indeed, the regression of already established tumors and their metastases upon induction of apoptosis by treatment with the CD44v6 peptides could be due to inhibition of Met/VEGFR-2 or another CD44v6-mediated survival signal that re-sensitizes tumor cells to apoptosis. Together, these data suggest a central role for CD44v6 signaling in metastatic spreading and maintenance of metastases in distant organs.

CD44v6 expression is restricted to proliferative tissues, but is up-regulated in a variety of cancers (reviewed in¹). This makes CD44v6 a prime target for cancer therapy. Humanized monoclonal blocking antibodies have been developed and were used in clinical trials (reviewed in²). However, previous approaches aimed at targeting the CD44v6 expressing cells via toxins or radionuclides. This was due to the lack of knowledge of its modulatory role as an integral signaling hub.

Nonetheless, despite promising activities at an early clinical stage, the CD44 targeting trials were stopped due to the death of one patient during a phase I dose escalation study with a CD44v6 antibody coupled to the cytotoxic drug mertansine (reviewed in²). Of note, radio-labeled antibodies demonstrated a favorable toxicity profile. From the current perspective, and the here presented data, targeting CD44v6 signaling rather than ablative approaches via delivery of toxins to CD44v6 expressing tumors may constitute a more promising and least toxic strategy.

The fact that the CD44v6 peptide not only interferes with the metastatic spreading of tumor cells but even leads to regression of already established metastases makes it a very promising tool for cancer therapy, particularly for treatment of pancreatic cancer, the fifth leading cause of cancer death. In fact, the five years survival rate in the range of 3-5% is the lowest amongst all cancers, the main reason being the aggressive metastatic potential of this cancer type. Gemcitabine monotherapy and more recently approved chemotherapy combinations FOLFIRINOX and nabPaclitaxel-gemcitabine only modestly improve survival in advanced pancreatic cancer.

The critical role of HGF/Met in carcinogenesis prompted the development of tools such as Met or HGF inhibitors to interfere with the malignant processes³⁻⁵. Unfortunately all these tools were not as successful in the clinics as suggested by the animal experiments. This lack of success might be due to the fact that targeting only one protein is not sufficient. To substantially impact the treatment of pancreatic cancer patients development of novel rationally designed multimodal therapy strategies are urgently needed. An advantage of the CD44v6 peptide for therapy is that it targets not only Met activation but also that of other RTKs relevant for tumorigenesis, such as VEGFR-2 and thereby interferes as well with angiogenesis⁶. In this regard it is interesting that the metastatic spreading of pancreatic islet in the RIP-Tag2 mice is decreased when the animals were treated not only with VEGFR inhibitors but in addition also with Met inhibitors⁷. Simultaneous inhibition of tumor cell centric phenomenon such as cell viability and invasiveness as well as blockade of tumor angiogenesis by CD44v6 neutralizing peptide may therefore provide a powerful dual strategy to combat the intricate processes involved in formation and growth of metastatic lesions.

Synthetic inhibitors have been developed that target simultaneously Met and VEGFR-2. One of these compounds, Cabozantinib is already FDA-approved⁸. Cabozantinib, demonstrated encouraging randomized Phase II data⁹. However, despite improved progression-free-survival no significant overall-survival benefit was

found after Cabozantinib treatment of castration-resistant metastatic prostate cancer patients as compared to prednisone control arm in the COMET-1 phase III trial (<http://ir.exelixis.com/phoenix.zhtml?c=120923&p=irol-newsArticle&ID=1962549>). A drawback of these inhibitors is that they very often induce drug resistance and side effects. CD44v6 and Met-expressing tumor cells are protected against drug-induced apoptosis¹⁰. Thus, the CD44v6 peptide might protect against drug resistance in combination regimen.

CD44 has been identified as a bona fide stem cell marker on many cancer types including pancreatic carcinoma¹¹. Only in few cases, however, the specific CD44 isoform that correlates with stemcellness has been identified. One such case is breast cancer where a CD44v6⁺/CD24^{low} population of cells has stem-cell characteristics¹². CD44v6 has also been described as a stem cell marker for colorectal cancer¹³ where it is involved in the maintenance of stemcellness and pancreatic tumors¹⁴. High Met-expression was also detected on populations of cancer stem cells, e.g. in head and neck squamous cell carcinoma¹⁵. Particularly interesting is the finding that Met and CD44 are stem cell markers on pancreatic carcinoma¹⁶ suggesting that the co-receptor function of CD44 for Met might be of functional importance in these cells. Of note, an antibody against CD44, claimed however to recognize CD44s only, was shown to inhibit pancreatic tumor initiation¹⁷.

The fact that already established metastases can be eliminated by treatment with CD44v6-specific peptides demonstrates that CD44v6 is required for the growth and maintenance of metastases at least in part via its co-receptor function. In line with our observation, the requirement of CD44v6 and Met for the metastatic spreading of colorectal cancer was recently reported¹⁸. Additionally, CD44v6 and Met could be also required for the preparation of the metastatic niche. CD44v6 expressing pancreatic carcinoma cells seem to prepare a pre-metastatic niche by sequestration of exosomes¹⁹ and establishment of an extracellular matrix that allows growth and survival. Furthermore Met drives a genetic program that provides a fibrin matrix supporting cell proliferation and invasion²⁰.

In conclusion, we provide evidence for rationale design of CD44v6 targeting therapy to prevent- or eradicate pancreatic cancer metastasis. CD44v6 plays a critical role as co-receptor of key metastasis regulating signaling such as Met, VEGFR and potentially other, not hitherto discovered pathways. Therefore, this strategy may demonstrate some advantages over current single modality approaches. The superior efficacy compared to selective RTK inhibition suggests that CD44v6

targeting therapy may control multiple pathophysiological processes governing tumor invasion and metastasis.

Materials and Methods

Cell Lines

Rat pancreatic carcinoma cells BSp73AS (designated "AS") and transfectants have been described.⁷ Human pancreatic cancer cells L3.6pl were kindly provided by C. Bruns¹¹ (University of Magdeburg, Germany). FC1245 cells were thankfully obtained from D. Tuveson (Cold Spring Harbor Laboratory, Cold Spring Harbor, NY), and were cultured in RPMI 1640 (ATCC, Wesel, Germany) and 10% fetal calf serum (FCS). Panc1 cells (ATCC) were maintained in Dulbecco's modified Eagle medium and 10% FCS. Primary JoPaca-1 cells were kindly provided by Dr Hoheisel (Deutsches Krebsforschungszentrum, Heidelberg, Germany) and cultured in Iscove's modified Dulbecco's Medium (Life Technologies, Darmstadt, Germany) and 10% FCS.

Antibodies and Other Reagents

The monoclonal antibody VFF18 that specifically recognizes human CD44v6 was from Bender (Vienna, Austria), the anti-extracellular signal-regulated kinase (ERK)1 (K-23), Met (C-28), and Green Fluorescent Protein (GFP) antibodies (sc-101525) were from Santa Cruz Biotechnology (Heidelberg, Germany), the cleaved caspase-8 antibody (IMG-5703) was from Imgenex (San Diego, CA), the CD31 antibody (MEC13.3) was from BD Biosciences (Heidelberg, Germany), and the cleaved caspase-3 (Asp175), Phospho-Met (Tyr1234/1235) (D26), Met (25H2), and the phospho-ERK phospho-p44/42 antibodies were from Cell Signaling Technology (Beverly, England). The rat exon v6-specific antibody 1.1ASML has been described.¹² Secondary antibodies labeled with horseradish peroxidase were from Dako (Glostrup, Denmark). The Alexa Fluor R 546 goat anti-rabbit secondary antibody was from Life Technologies. HGF was from Peprotech (Hamburg, Germany). The rv6pep (KEKWFENEWQGKNP), mv6pep (QETWFQNGWQGKNP), and hv6pep (KEQWFGNRWHEGYR) have been described.^{8 and 9} Solubility of hv6 pep is 15 mg/mL in phosphate-buffered saline, and 16 mg/mL for rv6pep. Half-life in serum for hv6pep is 11 minutes, and 55 minutes for the first degradation product, a 12mer containing the critical amino acids that suffice for inhibition (Supplementary Figure 1). Here, we used the 14mer peptides, but all experiments also were repeated with 5mer peptides and provided similar results. For in vivo imaging experiments the rat 11mer WFENEWQGKNP, the mouse (WFQNGWQGKNP), and human (WFGNRWHEGYR) 11mer were labeled with the fluorescent dye DY681. The hv6pep was used as a control peptide in the rat model, and rv6pep was used in the human and mouse orthotopic tumor models. Peptides were from Bachem

(Bubendorf, Switzerland) or Intavis (Köln, Germany). Lyophilized peptides were resuspended in phosphate-buffered saline.

Animal Experiments

Male athymic nude mice (NCI-nu) were purchased from Harlan (Roßdorf, Germany). BDX rats were bred in house. Animals were housed and maintained under specific pathogen-free conditions in facilities approved by the Regierungspräsidium Karlsruhe. All animals were handled according to German regulations for animal experimentation. Experiments were authorized by the Regierungspräsidium (35-9185.817G-192/10 and 35-9185.817G-106/09). *LSL-Kras^{G12D}*, *LSL-Trp53^{R172H}*, and *Pdx1-Cre* (KPC) mice have been described previously.¹³

Patient Samples

All studies were approved by the Ethics Committee of the University of Heidelberg in Germany, and written informed consent was obtained from all patients. Biopsy specimens were immediately collected, snap-frozen in liquid nitrogen, and stored at -80°C.

Additional information on animal experiments and protocols for immunoblotting, lentiviral transfection of short hairpin RNA (shRNA), cell migration assay, quantitative determination of HGF and VEGF, serum stability, in vivo fluorescence imaging, histology, immunofluorescence, and transcriptome analysis of patient samples can be found in the Supplementary Materials and Methods section.

References

1. Naor D, Nedvetzki S, Golan I, et al. CD44 in cancer. *Crit Rev Clin Lab Sci* 2002;39:527-79.
2. Orian-Rousseau V, Ponta H. Perspectives of CD44 targeting therapies. *Archives of toxicology* 2014.
3. Cecchi F, Rabe DC, Bottaro DP. Targeting the HGF/Met signaling pathway in cancer therapy. *Expert opinion on therapeutic targets* 2012;16:553-72.
4. Gherardi E, Birchmeier W, Birchmeier C, et al. Targeting MET in cancer: rationale and progress. *Nature reviews. Cancer* 2012;12:637.
5. Mazzone M, Basilico C, Cavassa S, et al. An uncleavable form of pro-scatter factor suppresses tumor growth and dissemination in mice. *The Journal of clinical investigation* 2004;114:1418-32.
6. Tremmel M, Matzke A, Albrecht I, et al. A CD44v6 peptide reveals a role of CD44 in VEGFR-2 signaling and angiogenesis. *Blood* 2009;114:5236-44.
7. You WK, Sennino B, Williamson CW, et al. VEGF and c-Met blockade amplify angiogenesis inhibition in pancreatic islet cancer. *Cancer research* 2011;71:4758-68.
8. Yakes FM, Chen J, Tan J, et al. Cabozantinib (XL184), a novel MET and VEGFR2 inhibitor, simultaneously suppresses metastasis, angiogenesis, and tumor growth. *Molecular cancer therapeutics* 2011;10:2298-308.
9. Smith MR, Sweeney CJ, Corn PG, et al. Cabozantinib in chemotherapy-pretreated metastatic castration-resistant prostate cancer: results of a phase II nonrandomized expansion study. *Journal of clinical oncology : official journal of the American Society of Clinical Oncology* 2014;32:3391-9.
10. Jung T, Gross W, Zoller M. CD44v6 coordinates tumor matrix-triggered motility and apoptosis resistance. *The Journal of biological chemistry* 2011;286:15862-74.
11. Dembinski JL, Krauss S. Characterization and functional analysis of a slow cycling stem cell-like subpopulation in pancreas adenocarcinoma. *Clinical & experimental metastasis* 2009;26:611-23.
12. Snyder EL, Bailey D, Shipitsin M, et al. Identification of CD44v6(+)/CD24- breast carcinoma cells in primary human tumors by quantum dot-conjugated antibodies. *Laboratory investigation; a journal of technical methods and pathology* 2009;89:857-66.
13. Todaro M, Gaggianesi M, Catalano V, et al. CD44v6 Is a Marker of Constitutive and Reprogrammed Cancer Stem Cells Driving Colon Cancer Metastasis. *Cell stem cell* 2014;14:342-56.
14. Gaviraghi M, Tunici P, Valensin S, et al. Pancreatic cancer spheres are more than just aggregates of stem marker-positive cells. *Bioscience reports* 2011;31:45-55.
15. Sun S, Wang Z. Head neck squamous cell carcinoma c-Met(+) cells display cancer stem cell properties and are responsible for cisplatin-resistance and metastasis. *International journal of cancer. Journal international du cancer* 2011;129:2337-48.
16. Li C, Wu JJ, Hynes M, et al. c-Met is a marker of pancreatic cancer stem cells and therapeutic target. *Gastroenterology* 2011;141:2218-2227 e5.
17. Li L, Hao X, Qin J, et al. Antibody against CD44s inhibits pancreatic tumor initiation and postradiation recurrence in mice. *Gastroenterology* 2014;146:1108-18.
18. Todaro MC, Khandheria BK, Paterick TE, et al. The practical role of echocardiography in selection, implantation, and management of patients requiring LVAD therapy. *Curr Cardiol Rep* 2014;16:468.
19. Jung T, Castellana D, Klingbeil P, et al. CD44v6 dependence of premetastatic niche preparation by exosomes. *Neoplasia* 2009;11:1093-105.
20. Boccaccio C, Sabatino G, Medico E, et al. The MET oncogene drives a genetic programme linking cancer to haemostasis. *Nature* 2005;434:396-400.
21. Bruns CJ, Harbison MT, Kuniyasu H, et al. In vivo selection and characterization of metastatic variants from human pancreatic adenocarcinoma by using orthotopic implantation in nude mice. *Neoplasia* 1999;1:50-62.

Acknowledgments

We are very grateful to Christiane Bruns (University Hospital, Magdeburg, Germany) for kindly providing the L3.6pl cells. We thank Silvia Giordano (University of Turin, Turin, Italy) for the lentiviral system. We would like to thank David Tuveson (CSH, NY, USA) for kindly providing the FC1245 cells. We are very thankful to Selma Huber and the animal facility of the Institute of Toxicology and Genetics for tremendous help with the animal experiments as well as Giuseppina Pace, Sarah Greco and Viviane Lobstein and for excellent technical assistance. This work was supported by grants of the Deutsche Forschungsgemeinschaft (OR 124/4-1 and 2).

Figure legends

Figure 1. The CD44v6 co-receptor function for Met is required for tumor metastasis.

A Top: CD44 constructs for transfection of AS cells. Bottom: AS cells and transfectants were induced with HGF where indicated and Met/ERK activation was determined. Numbers refer to the fold induction as calculated by the computer program ImageJ. Experiments were performed at least three times and gave similar results.

B Left: Cells used in A were subcutaneously injected into the posterior flank of syngeneic rats. Pictures represent axillary lymph nodes and lungs isolated four weeks after implantation. Arrows indicate metastases. The number of animals used is given in Table 1. Right: Scheme representing the metastatic behavior of transfectants. Quantification of the average number of metastases.

C Immunohistochemical analysis of ASv6 tumors infected with lentivirus expressing ctrl shRNA or Met shRNA. Sections were stained with an anti-GFP antibody to monitor shRNA-transduced areas or with a phospho-Met antibody. A representative picture is shown. Ten animals per group (Table 1) were analyzed. Magnification 20x.

Figure 2. A CD44v6 specific peptide blocks metastasis of rat tumor cells.

A ASv6 cells were induced with HGF in the presence of rv6pep, a CD44v6 specific antibody (1.1ASML) or a control peptide (mouse) as indicated. Met, ERK and Akt

activation was determined using phospho-specific antibodies. Numbers refer to the fold induction.

B ASv6 cells were injected subcutaneously into the right posterior flank of BDX rats. Average tumor volume in rats treated as indicated was determined at the end of the experiments. The group size is given in Table 1 and 2.

C Pictures represent axillary lymph nodes and lungs. Treatment with the rv6pep (i.v.), the control peptide or the CD44v6 antibody started one week after implantation. Arrows indicate metastases. The group size is given in Table S2.

D Top: Chart showing the average number of metastases. Bottom: Representative lung sections of animals treated with rv6pep or with the control peptide stained with H&E and PAS are shown. Magnifications 1,5x, 4,5x and 20x.

Figure 3. A CD44v6 peptide prevents metastasis of mouse tumor cells in a pancreatic cancer orthotopic model.

A FC1245 cells were induced with murine HGF after incubation with mv6pep, a control peptide (rat; both 0,025 μ M) or Crizotinib (0,5 μ M) as indicated. Met and ERK activation was determined using phospho-specific antibodies. Numbers refer to fold induction.

B FC1245 cells were injected orthotopically into the pancreas of male C57BL/6 mice as described²¹. One week later animals were injected i.p. with mv6pep or control peptide (20 μ g). Injection was repeated three times per week. Crizotinib was applied daily orally at 25 mg/kg. Animals were killed 14 days after beginning of the treatment. Average tumor volume at autopsy is represented.

C Top: Organs of the animals in B at autopsy were examined for macroscopic metastases. A representative picture is shown. Bottom: Graph representing the liver metastases number.

D Top: H&E staining of tumors isolated from animals treated either with mv6pep, control peptide or Crizotinib (left). Representative immunofluorescence stainings of primary tumors for phospho-Met (middle) and Met (right). Nuclei are stained with DAPI. Bottom: Quantification of phospho-Met in the primary tumor.

E Kaplan-Meier survival analysis of tumor-bearing KPC mice treated three times per week with either mv6pep (red line, n = 5) or control peptide (blue line, n = 5). P values, Log Rank.

Figure 4. A CD44v6 peptide interferes with metastasis of human tumor cells in a pancreatic cancer orthotopic model.

A L3.6pl (left) or JoPaca-1 (right) cells were treated with hv6pep or the control peptide (rat) prior to induction with HGF. Met, ERK and Akt activation was determined in western blot. The experiment was repeated at least five times.

B Body weight determination of animals injected with JoPaca-1 cells and treated with hv6pep or control pep.

C L3.6pl or JoPaca-1 cells were injected orthotopically into the pancreas of male nude mice. One week later animals were injected i.p. with hv6pep or control peptide (20 µg). Injection was repeated three times per week. Animals were killed at the indicated days. The quantification represents the average tumor volume of animals treated either with hv6pep or the control peptide at the end of the experiment. Tumors were stained for CD44v6 (VFF18). A representative picture is shown. Nuclei were stained with hematoxylin (L3.6pl). Analysis of five animals per group gave similar results.

D Top: Macroscopic liver and kidney metastases from hv6pep or control peptide treated animals of the experiment in C. Bottom: Bars show the average number of metastases.

E Top: Expression of CD44 transcripts in pancreatic cancer patients. Patient samples were clustered into two groups according the expression levels of v6 containing transcripts (v6 high Up, red) vs. v6 low (Down, blue) groups. Bottom: Boxplot showing the relative increase in expression of Met in v6 Up group compared to the v6 Down group. Relative Met expression (log2) to the median of the v6 down cohort are presented. The patient group with high CD44v6 expression has a ~ four-fold increase in median expression of MET (p=0.01, adjusted Bonferroni).

F A significant decrease in median overall survival (~13 months) for patients with high expression levels of v6 transcripts (red line) compared to patients with low expression of v6 transcripts (18 months, blue line) was found ($p=0.02$).

Figure 5. The CD44v6 peptide reduces metastasis more efficiently than small molecule inhibitors.

A The average tumor volume of mice ($n=5$) with orthotopic L3.6pl tumors is represented after three weeks treatment with the indicated compounds.

B Average number of metastases is represented in a graph. White arrows on pictures indicate metastases.

C Representative H&E staining of liver sections after three weeks of treatment.

Figure 6. Reversion of pre-existing metastases by the CD44v6 peptide.

A Schematic representation of the experimental procedure. ASv6 cells were injected in rats. Treatment with rv6pep or control peptide (mouse) started after three weeks. After 21 additional days the animals were sacrificed and analyzed for lung metastases. The quantification represents the average number of metastases. The group size is given in Table S6.

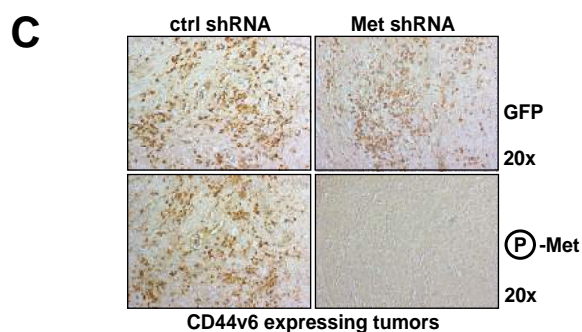
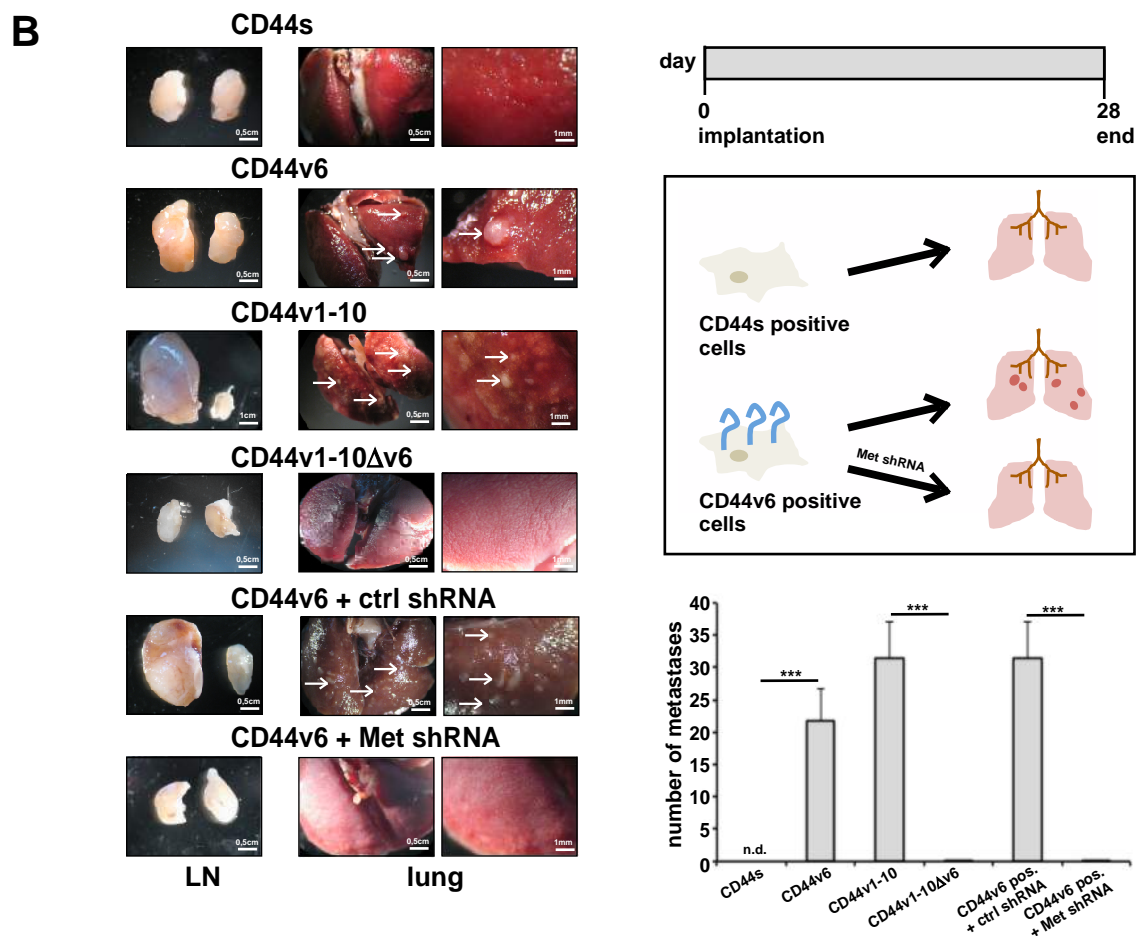
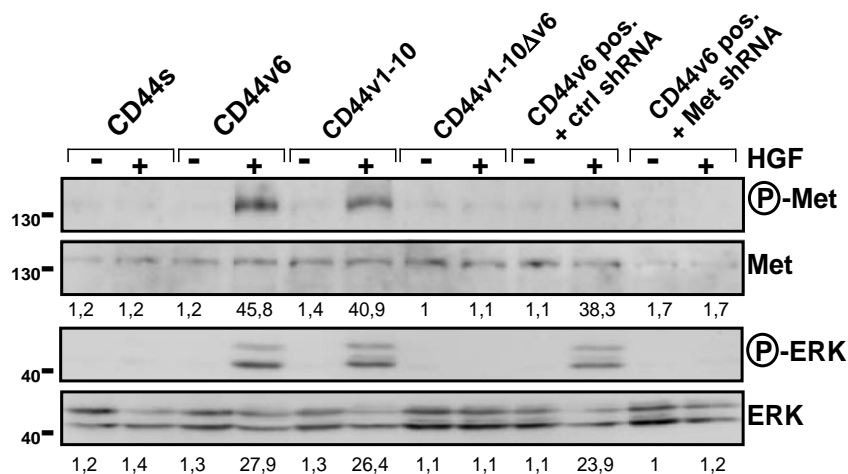
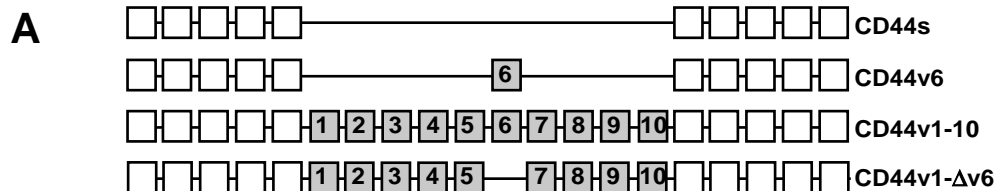
B Schematic representation of the experimental procedure. L3.6pl were injected in mice. Representative pictures of livers from tumor-bearing mice treated with hv6pep or control peptide (rat). Arrows indicate metastases. The quantification shows the average number of metastases. The group size is given in Table S3.

C Schematic representation of prolonged survival of animals receiving hv6pep. Bar chart representing the average tumor size before treatment start, after end of treatment with hv6pep for 35 days (hv6pep group1) and after 49 days without treatment (hv6pep group 2).

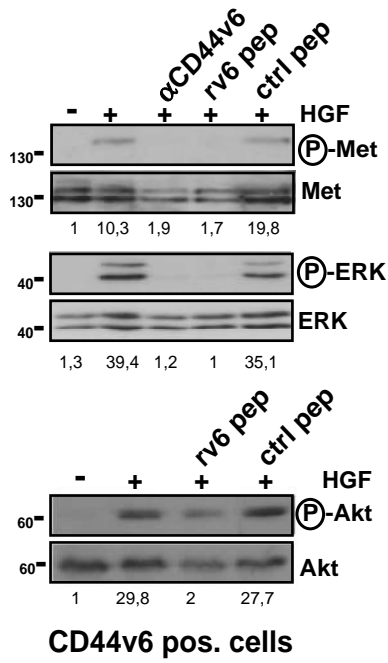
Figure 7. The CD44v6 peptide induces apoptosis in already established metastases.

Three weeks after injection of ASv6 tumor cells, animals received an injection of rv6pep or control peptide every second day. At the indicated days, one animal of each group was sacrificed. Apoptosis in lung was monitored using an antibody against cleaved Caspase-3 and cleaved Caspase-8. The area of the metastase is

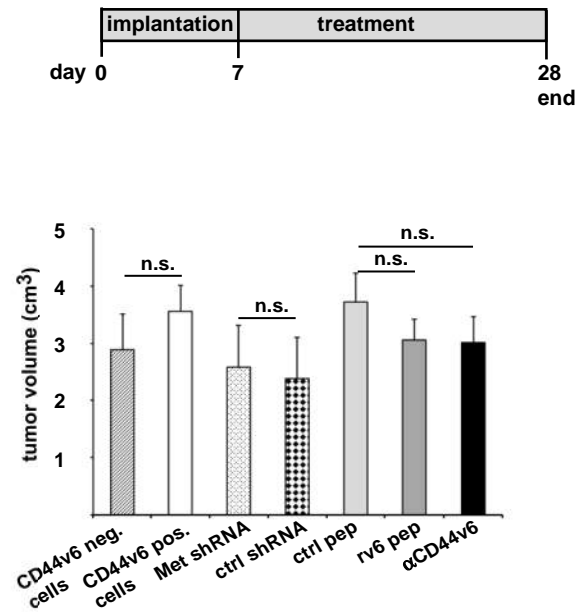
marked (M). The magnification is 4,5x. The experiment was performed two times with similar outcome.



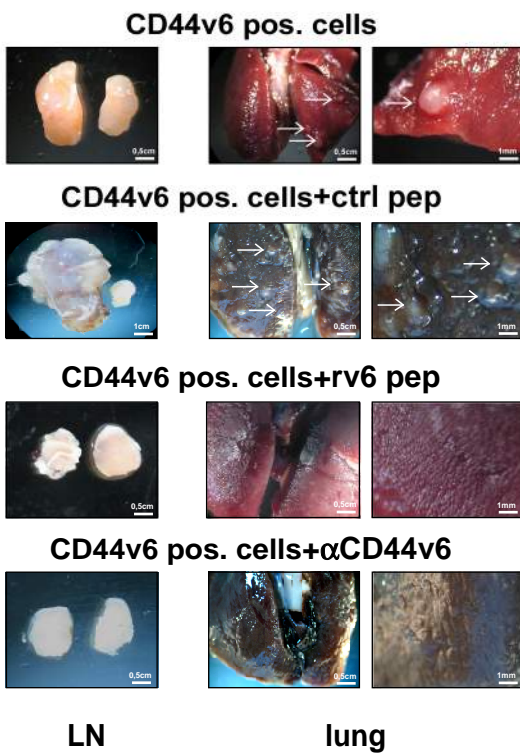
A



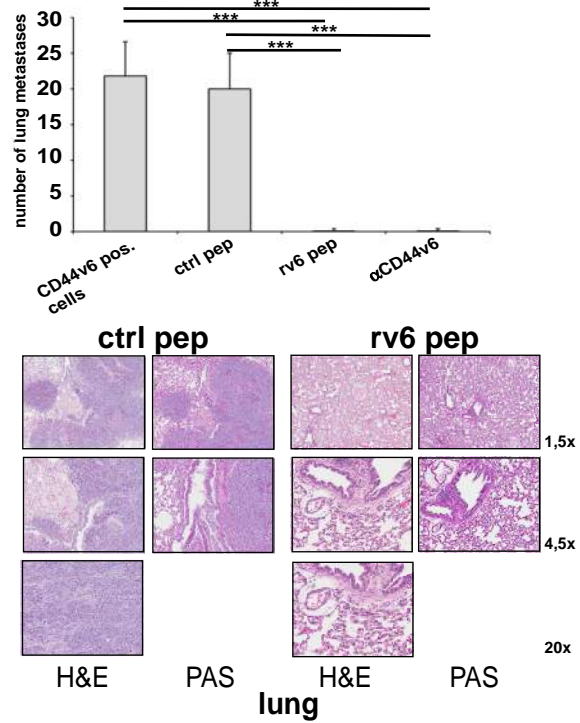
B

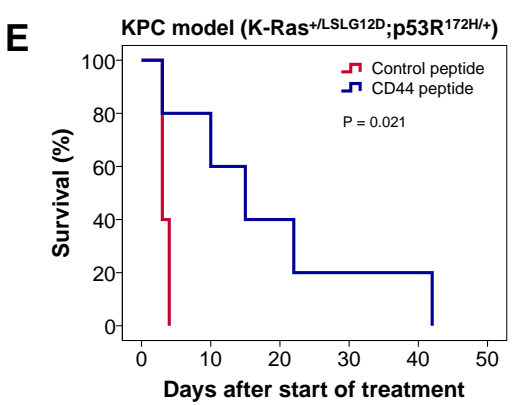
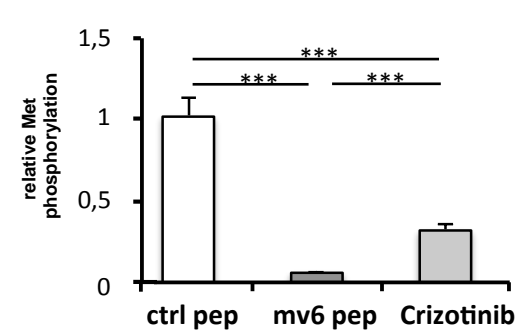
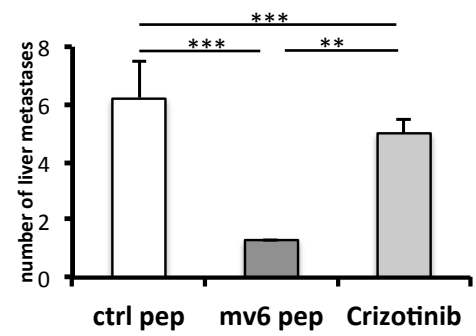
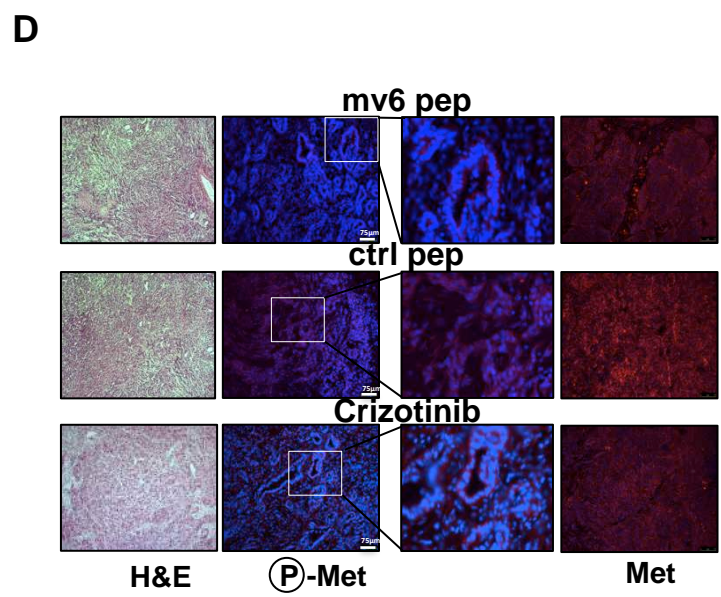
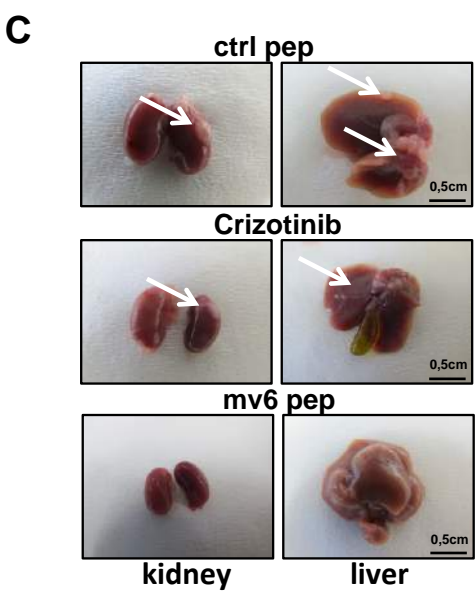
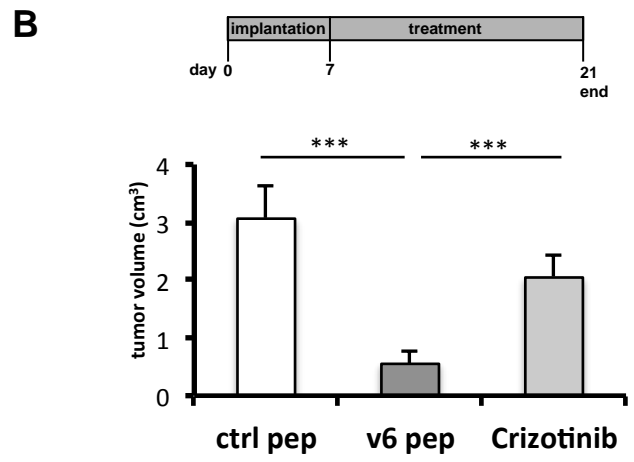
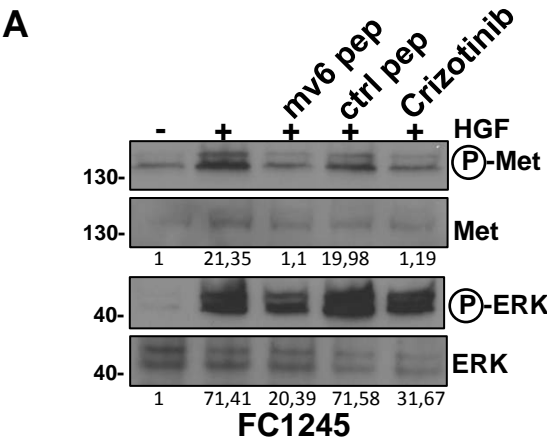


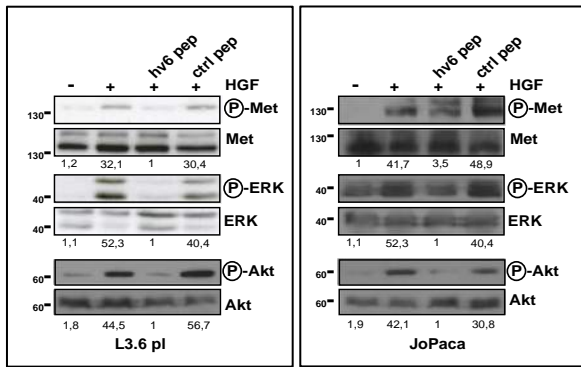
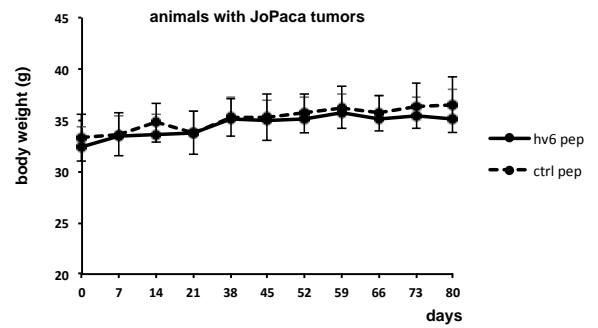
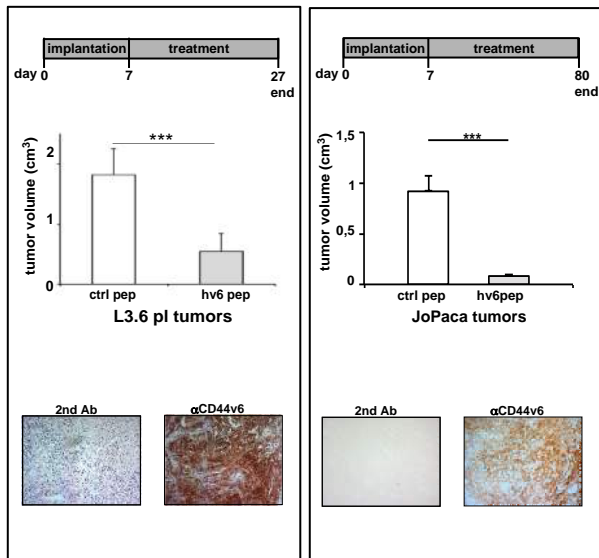
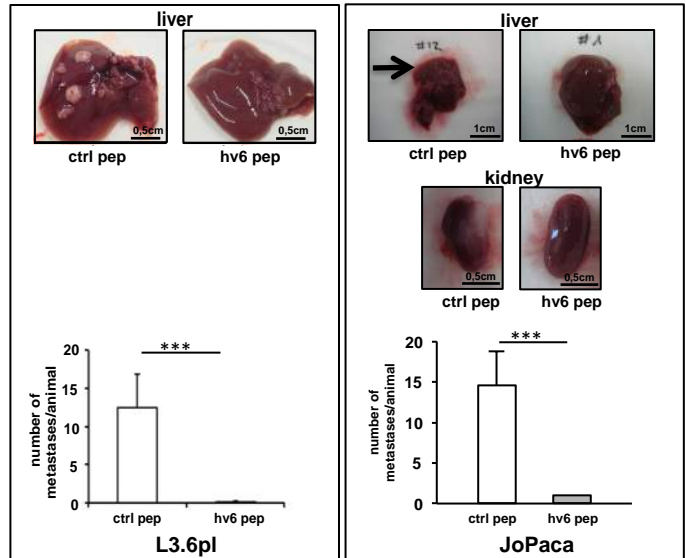
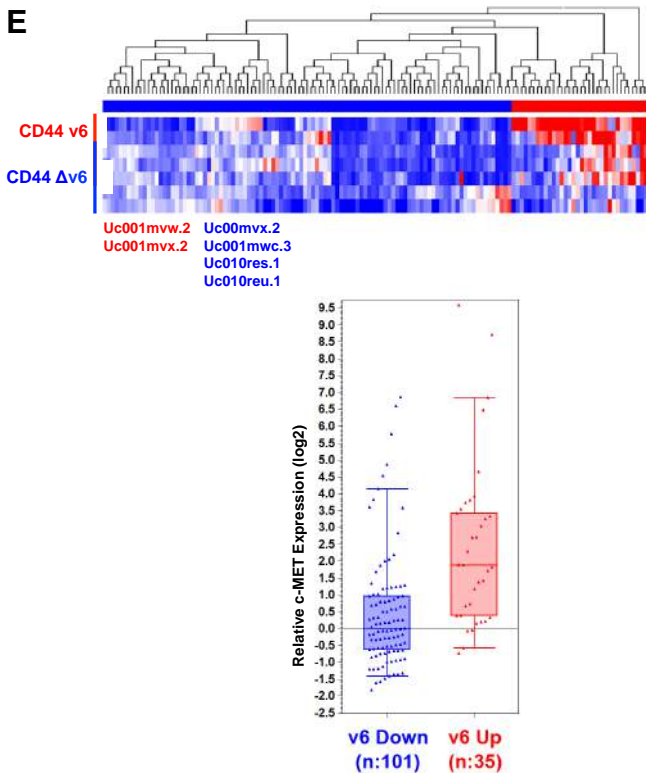
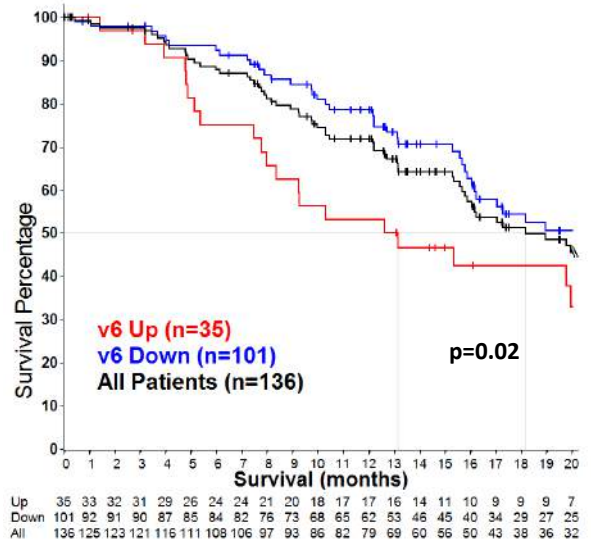
C

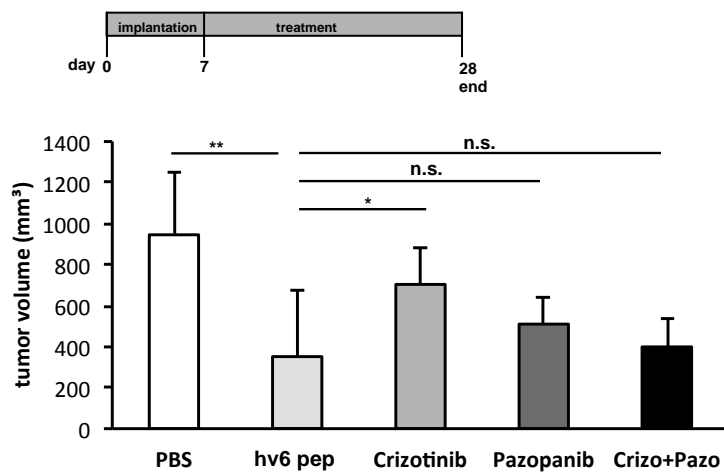
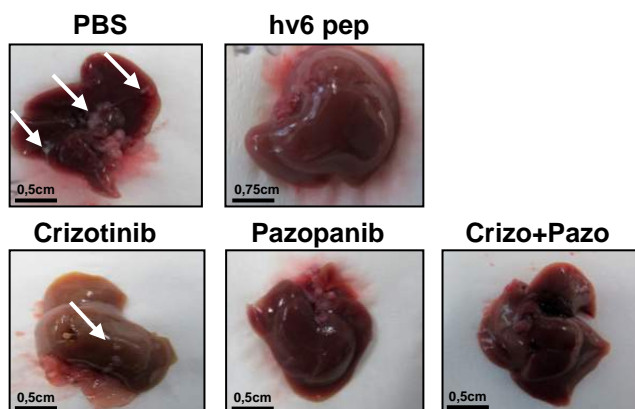
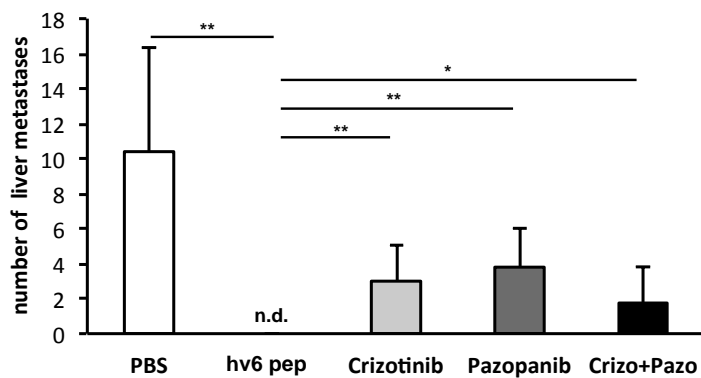
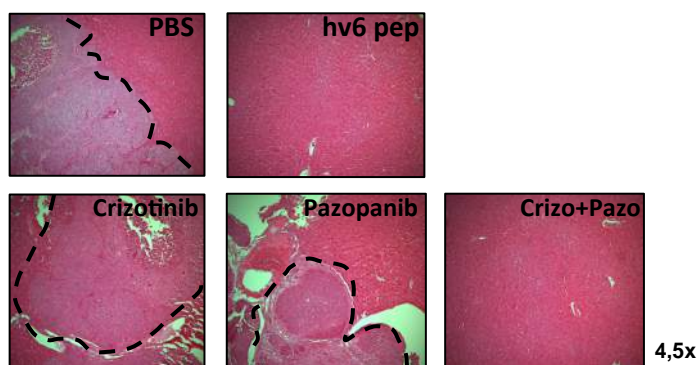


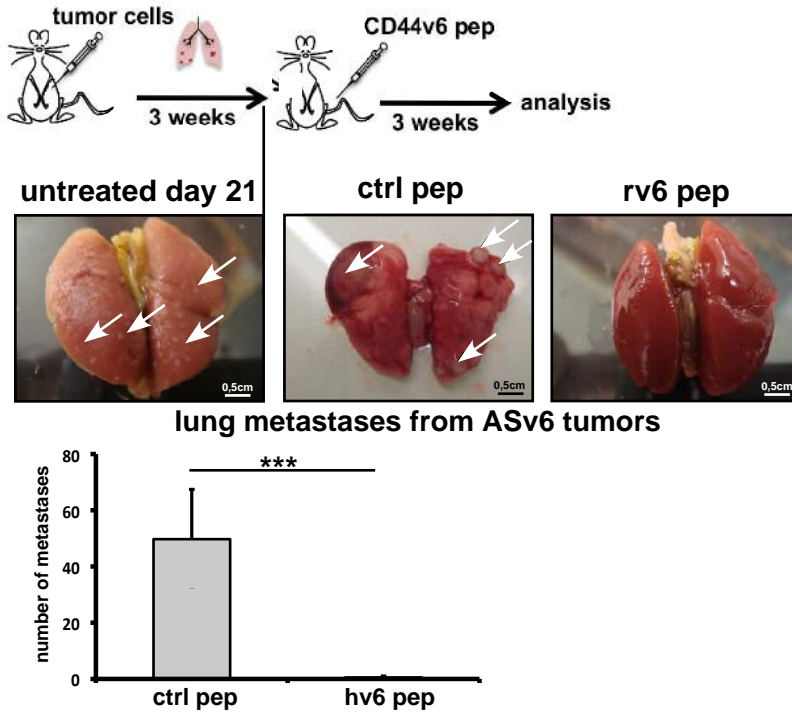
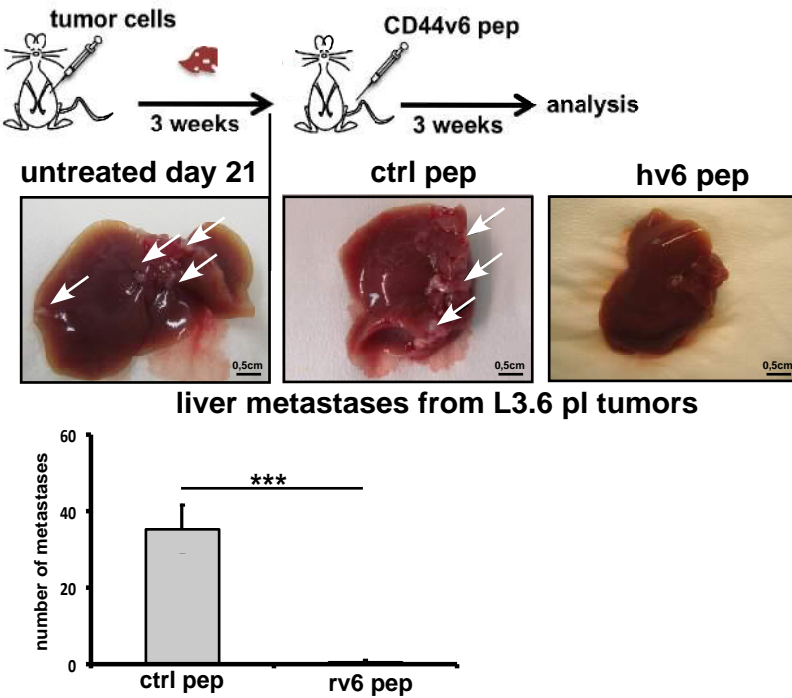
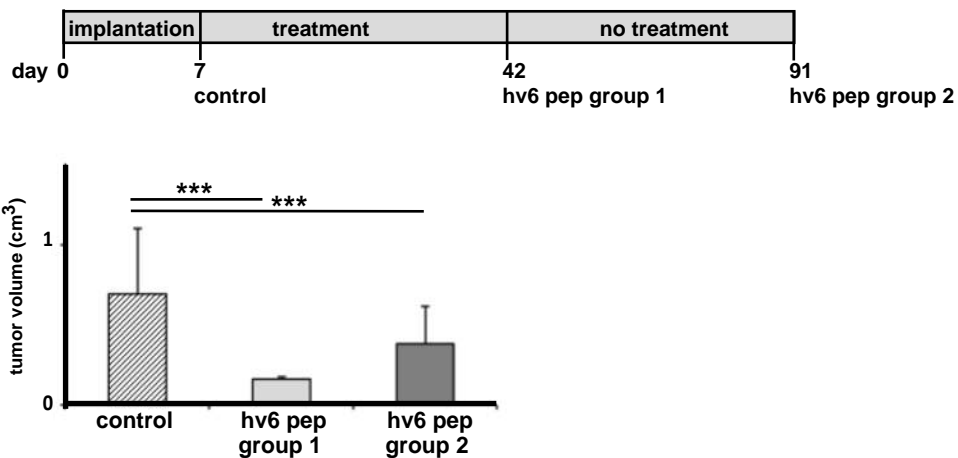
D

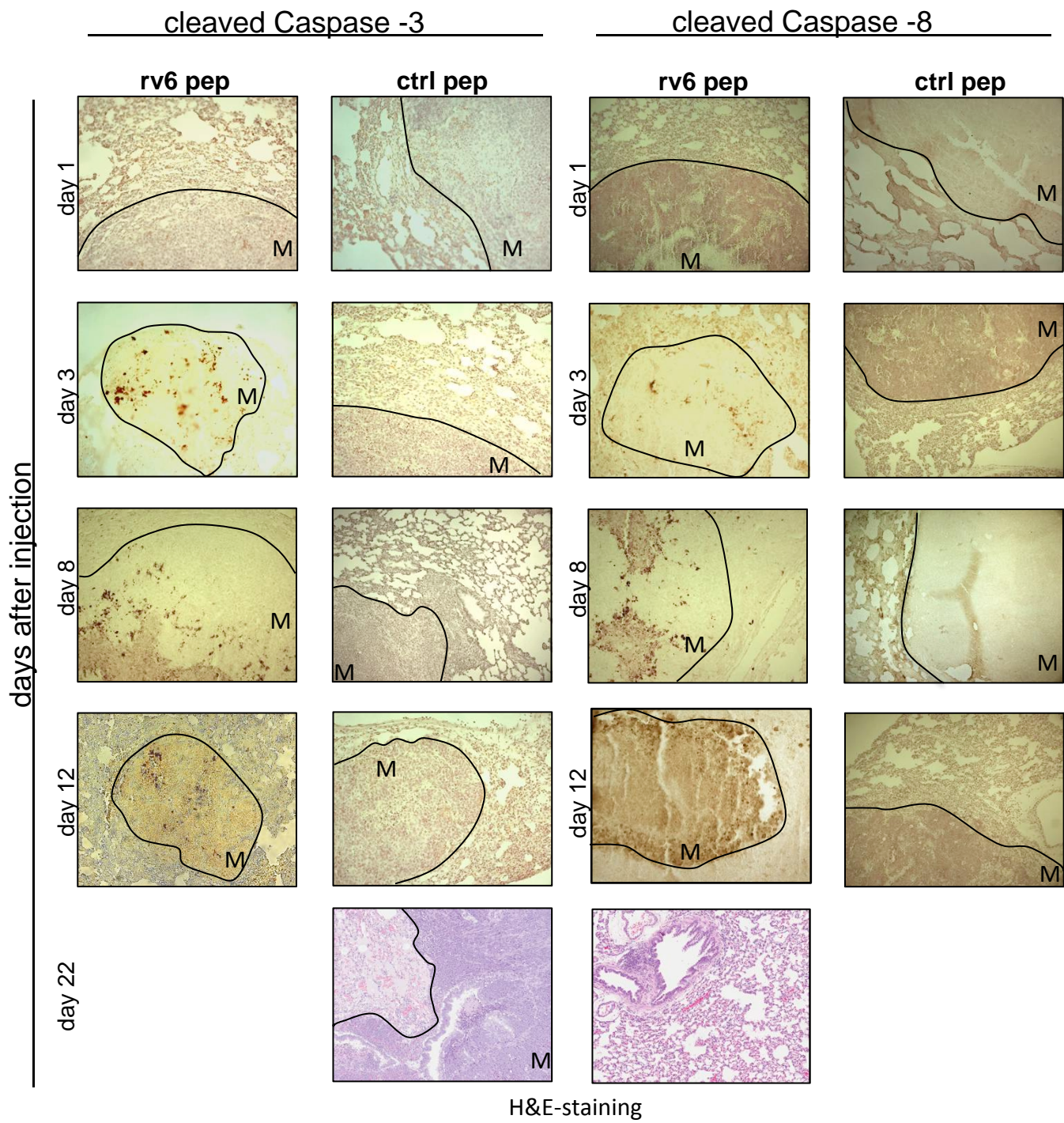




A**B****C****D****E****F**

A**B****C**

A**B****C**



Supplementary Materials and Methods

Lentiviral transfection of shRNA

The lentivirus system used for silencing Met has already been described¹².

Western Blot (WB) analysis

Serum-starved cells (24 hours) were induced with HGF (10 ng/ml) at 37°C for 5 minutes. Where indicated, cells were treated with peptides (100 ng/ml) prior to induction at 37°C, 10 minutes. Cells were then lysed in SDS-sample buffer containing 100 mM DTT, boiled and subjected to WB analysis. The intensity of the WB bands was quantified with the program Image J (National Institutes of Health).

CellPlayer™ 96-well kinetic cell migration assay

The effect of mv6pep and Crizotinib on cell migration was assessed using FC1245 cells. Cells were grown to confluency in 96 well Essen ImageLock plates (Essen Bioscience, Ann Arbor, USA). Precise wounds were created in all wells of the 96 well plate using a 96-pin Wound Maker. Cells were gently washed and treated for 2 hours with PBS (vehicle), increasing concentrations of v6pep (0.025µM-0.5µM), and Crizotinib (0.5µM). Plates were placed inside the IncuCyte ZOOM imaging system (Essen Bioscience) and scans were made every 2 hours. Wound confluence metrics were quantified and analyzed with IncuCyte software.

Quantitative determination of human HGF and VEGF in cell culture supernatant

Human HGF and VEGF levels in cell culture medium of L3.6pl cells were detected using the Quantikine Human HGF Immunoassay and Quantikine Human VEGF Immunoassay from R&D Systems (Wiesbaden, Germany). 3×10^6 cells were cultured for 5 days in a 15 cm plate with hv6pep. Assays were performed according to manufacturer's instructions.

Serum stability of peptide

Stability of a of EQWFGNRWHEGY in human serum (Sigma-Aldrich, Taufkirchen, Germany) at 37 °C. Samples were taken after the individual incubation times, precipitated with the twofold volume of acetonitrile; the supernatant (7µL) was analyzed by HPLC (5 min 0-50% acetonitrile/water, 0.1% TFA, 2mL/min, Merck Millipore Chromolith Performance RP-18e 100-3 mm, ambient temperature). The degradation proceeds via multiple intermediates, for example EQWFGNRWHE, EQWFGNRW or FGNRWHE was detected by LCMS.

Animal experiments

For the rat syngeneic model, 1×10^6 cells were subcutaneously injected into the right posterior flank of the animals. Tumors developed for four weeks. During this time period animals injected with ASv6 cells expressing Met shRNA or control shRNA received doxycycline in drinking water. At the end of the experiment, primary tumors were isolated. Lungs and axillary lymph nodes were analyzed. The tissues were fixed in 4% Formalin and embedded in paraffin for analysis. Where indicated animals received 200 µg of peptide or antibody per i.v. or i.t. injection three times per week for four weeks. Treatment of rats with a hundred fold higher single dose of peptide showed no acute toxicity (study performed at LPT Hamburg, Germany, study protocol available upon request). Tumor growth was monitored weekly using a caliper. Animals were killed at day 30 after start of the treatment.

For the human orthotopic model, L3.6pl cells (passage 24-26) were suspended in Hank's balanced salt solution (Invitrogen) after trypsinization. The cells were injected into the pancreas of male nude mice as described¹⁵. Mice were injected i.p. 7 days later with hv6pep respectively control peptide (20 µg). The injection was repeated three times per week for 21 days. i.p. injection was used instead of i.v. or i.t. as in rats since thrice weekly i.v. injection in mice is technically problematic. Two days after the last treatment animals were killed. The orthotopic implantation of Panc1 cells was performed accordingly. For the syngeneic FC1245 model, B6 mice were shaved prior to implantation of 5×10^5 cells. Treatment was performed with 20µg of mv6pep respectively control peptide (rat) thrice weekly.

JoPaca-1 cells (low passage) were injected orthotopically in the pancreas as described (Fredebohm et al., PloS one, 2012). Animals were treated for 80 days with

20µg of hv6pep respectively control peptide (rat) thrice weekly. Of note, even the extended treatment of the animals for 10 weeks with the peptide in the JoPaca model had no impact on the body weight (Fig. 4B) demonstrating the negligible toxicity of the peptide.

Genetically engineered mice

LSL-Kras^{G12D}, *LSL-Trp53^{R172H}*, *Pdx1-Cre* (KPC) mice have been described previously (Hingorani et al., 2005). KPC mice on a mixed strain background were kept in conventional animal facilities and given access to standard diet and water *ad libitum*. All experiments were performed in compliance with UK Home Office guidelines under licence approved by the local ethics committee. Mice were genotyped by Transnetyx (Cordova, Tennessee, USA) and monitored at least 3 times per week. Mice were treated with 20µg mv6pep or control peptide 3 times per week by intraperitoneal injection. Mice at end-point were sacrificed as per institutional guidelines, and tissues harvested and fixed in 10% neutral buffered formalin.

To examine the regression of metastases, either ASv6 or L3.6pl, were implanted as described above. Tumor growth was allowed for three weeks. At that time all animals had developed metastases in the control group. Animals were then injected i.p. with 20 µg (L3.6pl model: hv6pep or control peptide) or i.v. with 200 µg (rat model: rv6pep or control peptide) of peptides three times per week. Animals were killed 23 days after the start of the treatment.

To investigate a prolonged survival with hv6pep in the L3.6pl model animals were orthotopically injected with tumor cells as described above. Average tumor volume was determined for control animals after one week. Then animals were treated with hv6pep as described for 35 days. Animals of hv6pep group 1 were sacrificed to determine the tumor size. The tumor size of animals of the hv6pep group 2 was determined after additional 45 days without treatment.

Tumors were measured using an electronic caliper. The volume was determined using the formula: volume = length x width x length x 0,5. Standard deviations (SD) were calculated using Student's T-Test (*p<0,05, **p<0,01, ***p<0,001).

In vivo imaging using Optix MX2

In vivo imaging of the subcutaneously grown ASv6 tumors in BDX rats was performed using the near infrared fluorescence (NIRF)-imaging system Optix MX2 (ART, Montreal, Canada). To avoid autofluorescence of fur, rats were shaved around the tumor. Subsequently, animals were anesthetized using 2% isoflurane and gently fixed on the devices' warm plate for the entire time of data acquisition. To reduce fluorescence background, rats were fed with chlorophyll-reduced food (Provimi Kliba AG, Kaiseraugst, Switzerland) for one week prior NIRF imaging. All *in vivo* analyses were preceded by native scans of animals without any injection of the fluorescent probe. Rats were injected with 200 µg rv6pep DY681 or mv6pep DY681 (control) via the tail vein. Data were acquired at the indicated time after injection of the peptides. For *ex vivo* monitoring animals were sacrificed after 24 hours after peptide injection and tumor and organs of interest were scanned *ex vivo* using Optix MX2.

DY681 fluorescence was measured using excitation at 670 nm in combination with a 700 nm long-pass emission filter. Scans were performed with 1.5 mm raster, photon collection time of 0.5-1 s per scan point and varying laser power. Data sets were analyzed with OptiView (ART). Fluorescence intensity data are displayed in normalized counts (NC) where the measured fluorescence intensity (counts) was normalized for varying laser power and integration times, allowing comparison of measurements with different settings.

In vivo imaging using Pearl imager

In vivo imaging of the mice with the L3.6pl tumors was performed using the Pearl™ Imager (LI-COR Biosciences, Bad Homburg, Germany). The system uses two lasers (685 and 785 nm) for excitation and a charge-coupled device detector for signal detection. In order to standardize the images we made use of the Pearl Cam Software. Prior to imaging the mice were anesthetized with 2.0% isoflurane. Animals were placed on the warm plate of the imager and continuous delivery of isoflurane was achieved through a nose cone in the imaging drawer. Images were captured at white light, 700 and 800 nm. Animals were imaged prior to peptide injection and 24 hours after injection with either hv6pep DY681 or rv6pep DY681 as control. Immediately after each imaging session animals were killed, tumor, liver and spleen isolated and scanned *ex vivo*.

Immunofluorescence

ASv6 or L3.6pl cells were seeded at 5,000 cells/well of a Lab-Tek^R Chamber SlideTM (Nunc, Napierville, IL, USA). On the following day the cells were washed with cold PBS and fixed with 4% Formalin for 30 min at RT. Unspecific binding was blocked with 1% BSA in PBS for 1 hour at RT. The cells were incubated for 1 hour with the DY681-labeled peptides. After washing steps with PBS the cover slips were mounted with Fluorescence Mounting Medium (Dako, Glostrup, Denmark) and the immunofluorescence was measured by a laser scanning confocal microscope Leica TCS2 SP2 (Exton, PA, USA) and processed using Leica confocal software. A 20x objective was used for imaging.

Histology

For histo-morphological analysis paraffin-embedded sections of lungs were stained with H&E or PAS. Serial sections of whole tissue blocks were examined by analyzing sections every 20 µm; in each slice, presence and extension of metastatic deposit was assessed.

Immunohistological and immunofluorescence analysis

Paraffin sections were deparaffinized and rehydrated. For P-Met staining antigen unmasking was achieved by boiling the slides in 1 mM EDTA pH 8,0 followed by incubation for 15 min at a sub-boiling temperature, for CD31 staining the sections were treated with Proteinase K (8µg/ml) for 10 min at 37°C. For immunofluorescence staining of P-Met and P-VEGFR-2, blocking was performed with 5% goat serum (Dako) for 60 minutes. For immunohistochemistry endogenous peroxidases were at first blocked with 3% H₂O₂ in PBS followed by incubation with biotin blocking system (Dako) and then unspecific binding was inhibited by incubation with 5% FCS in PBS. The sections were incubated with the P-Met antibody, P-VEGFR-2 antibody, Met antibody, GFP antibody, CD31 antibody or VFF18 o/n at 4°C. PBS-washed sections were incubated with Alexa Fluor R 546 goat anti-rabbit or a biotinylated secondary antibody (for IHC-stainings rabbit anti-rat antibody for VFF18 and CD31, goat anti-rabbit for P-Met, cleaved Caspase-3 and cleaved Caspase-8 and rabbit anti-mouse

for GFP) for 45 minutes. For DAB staining the sections were treated with a streptavidin-peroxidase conjugate (Dako) and developed with DAB substrate system (Biozol, Eching, Germany). For immunofluorescence DAPI was used for nuclear staining.

RNA-seq in PDAC-Patients:

Genome-wide RNA-sequencing (RNAseq) based gene expression data were generated by TCGA consortium using Illumina HiSeq 2000 RNA Sequencing platform as previously documented [5] [1]. RNAseq data for 136 pancreatic ductal adenocarcinoma (PDAC) patients were obtained from the portal [<https://tcga-data.nci.nih.gov/tcga>] and the clinical characteristics is provided in the supplemental Table.. (xls). Level 3 RNASeq data contain expression quantification for genes, isoforms, exons and junctions. Isoform transcript quantification was analyzed separately in this study. The original method of quantification followed was the Reads Per Kilobase of exon model per Million mapped reads [8] The calculation of gene expression levels relied on the version 2 algorithm (RNASeqV2), i.e., for generation of level three data a combination of MapSlice and RSEM software packages for sequence assignment and estimation of sequence abundance was utilized [3,6,10]

Transcript-based analysis:

Annotation of transcripts:

Transcript IDs in the TCGA RNAseq data are annotated according to UCSC build 2009. The University of North Carolina – Chapel Hill online directory provides TCGA related files that are necessary for our analysis:

- First, to identify which transcripts IDs detect CD44 expression, the file ``https://webshare.bioinf.unc.edu/public/mRNAseq_TCGA/rsem_ref/unc_knownToLocus.txt`` was retrieved. In brief, it links every UCSC transcript ID to the corresponding gene of interest. 11 transcripts in total were assigned to CD44.
- The sequences for each of these transcripts were retrieved from ``https://webshare.bioinf.unc.edu/public/mRNAseq_TCGA/rsem_ref/hg19_M_rC_RS_ref.transcripts.fa``

Identification of transcripts of interest:

In our previous paper[7], a three amino acid sequence within the v6 sequence which was identified by mutational analysis to be essential for the co-receptor function of c-met and HGF. The sequence was RWH in humans. To identify which transcripts in the TCGA contain the v6 sequence, we used ExPASy [2] to translate the mRNA sequence of each transcript (11 in total) into amino acids. Only two transcripts, uc001mvv.2 and uc001mvu.2 were found to encode for the RWH amino acid sequence and therefore, were considered to be v6 containing/surrogates for v6 expression. Other transcripts lacking the critical v6 region were considered CD44 delta v6.

Data pre-processing:

The SUMO software package, developed in house, was used for data pre-processing ``<http://angiogenesis.dkfz.de/oncoexpress/software/sumo/>``. In brief, three steps of further processing were performed to RNAseqV2 data before analysis. Four transcripts with more than 20% zero values were filtered from our analysis (uc001mvy.2, uc009ykh.2, uc010rer.1, uc010ret.1). Pre-processing included virtual pool normalization of expression data for each individual transcript. Hierarchical clustering was performed using Chebyshev distance and complete linkage. Kaplan-Meier survival estimates were employed to examine potential differences in survival between patients who clustered to have a higher tumor expression of v6-containing transcripts (v6 Up) versus patients with a lower tumor expression of v6-containing transcripts (v6 Down). A p-value <0.05 by Log rank-test was considered statistically significant

Clinical characteristics:

The patient characteristics of the TCGA cohort are found in supplementary xls.file (X). Clinical data from the TCGA portal was downloaded and compiled into a matrix by an in-house software Table-Butler. The v6 Up and v6 Down patient groups were compared for differential enrichment in patient annotations by classical student's t-test, chi-square or Fisher's exact test where applicable. Patients in both groups were balanced for all demographic characteristics and treatment characteristics. In the v6 Up group, patients had significantly increased odds ratio of metastasis (44%) versus 23% of patients in the v6 down group (p=0.01).

Figure legends supplement

Figure S1. A CD44v6 specific peptide blocks tumor metastasis

Left: Top: Treatment scheme. Bottom: ASv6 cells were injected as described. After one week the animals were treated with rv6pep (i.t.) or PBS. Axillary lymph nodes (left) and lungs (right) were analyzed for metastases. The arrows indicate metastases. The animal number is given in Table 2.

Right: Bar chart representing the average number of metastases.

Figure S2. Binding of the CD44v6 peptide to primary tumors and metastases *in vivo*.

A Left side: ASv6 cells were induced with HGF in the presence of rv6pep DY681 respectively control peptide (mv6pep DY681) and ERK activation was measured. Right side: ASv6 cells were fixed and stained with the indicated peptides for one hour. Fluorescence and bright field images were taken using a laser scanning confocal microscope (Leica TCS2 SP2) with a 20x objective. The experiment was performed 2 times.

B Rats bearing a subcutaneous tumor of ASv6 cells were injected i.v. with 200 µg of indicated peptides and analyzed by NIRF imaging using Optix MX2 (ART, Montreal, Canada). Fluorescence intensities are displayed in normalized counts (NC). Series of fluorescent data sets obtained at the indicated time points after injection are shown. Red circle: Position of the tumor. The experiment was performed two times.

C Top: Rats bearing a subcutaneous tumor of ASv6 cells injected i.v. with 200 µg of indicated peptides. Bottom: Tumors and lungs were excised and fluorescence of the labeled peptides was monitored.

Figure S3: The CD44v6 peptide inhibits cell migration

A Phase-contrast images with the IncuCyte ZOOM imaging system of FC1245 cells from wells taken at different time points.

B Top: The wound closure was analyzed with IncuCyte software. Time-course of migration following treatment with PBS, different concentrations of mv6pep or Crizotinib. Bottom: Statistical analysis of the wound closure after twelve hours.

Figure S4. Specific accumulation of hv6pep in primary tumors and metastases of the L3.6pl human pancreatic cancer model.

A Left side: L3.6pl cells were induced with HGF in the presence of the indicated peptides and ERK activation was determined. Right side: L3.6pl cells were stained either with the hv6pep DY681 or rv6pep DY681. Images were taken with the laser scanning confocal microscope (Leica TCS2 SP2). This experiment was repeated two times. Magnification: 20x.

B L3.6pl tumors were orthotopically implanted for three weeks as has been described¹⁵ followed by one i.v. injection of the indicated peptides (20 µg). Binding of peptides was analyzed 24 hours after injection in anesthetized mice using the Pearl® Impulse Small Animal Imaging System (Li-Cor Biosciences). Each group consisted of three animals.

C Tumors, livers and spleens of all animals used in B were excised and fluorescence of the labeled peptides was monitored. Results for all animals were similar. The scales at the side indicate the synchronized signal intensity.

Figure S5. A Representative immunofluorescence staining of L3.6pl tumors from the hv6pep or control peptide treated animals for phospho-Met, Met and phospho-VEGFR-2. Analysis of five animals per group gave similar results.

B Human HGF and VEGF levels produced by L3.6pl cells in presence and absence of the hv6pep (200 ng/ml in the culture medium). Bars reflect average levels from triplicates obtained in three independent experiments.

C Staining of L3.6pl tumors for CD31. Magnification 50x. Graphs show the average vessel numbers respectively vessel size calculated from five tumors.

Figure S6. The v6 peptide reduces growth of Panc1 tumors

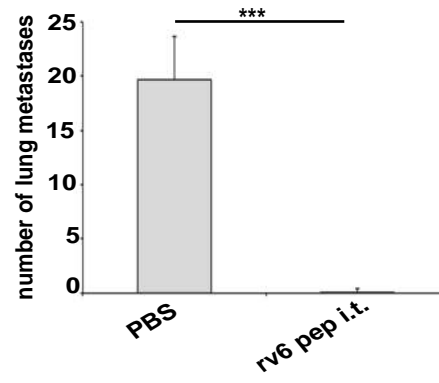
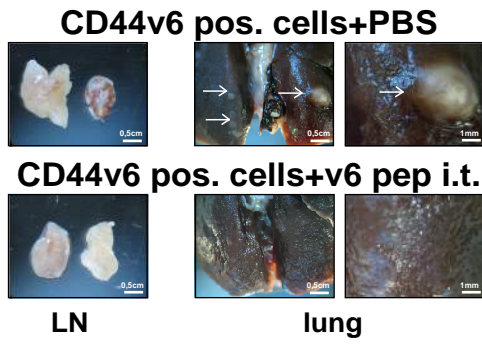
A Panc1 cells were treated with hv6pep or control pep (rat) prior to induction with 10 ng/ml HGF. Met and ERK activation were determined in western blot.

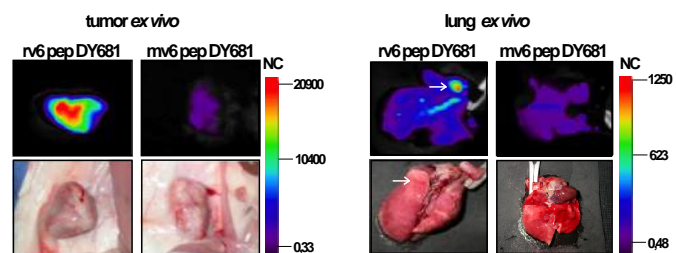
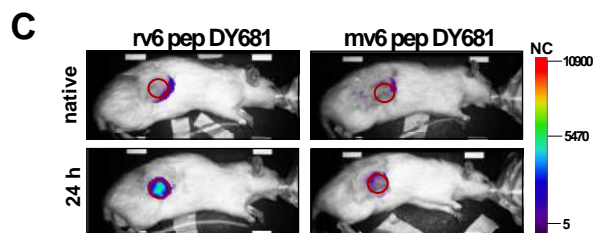
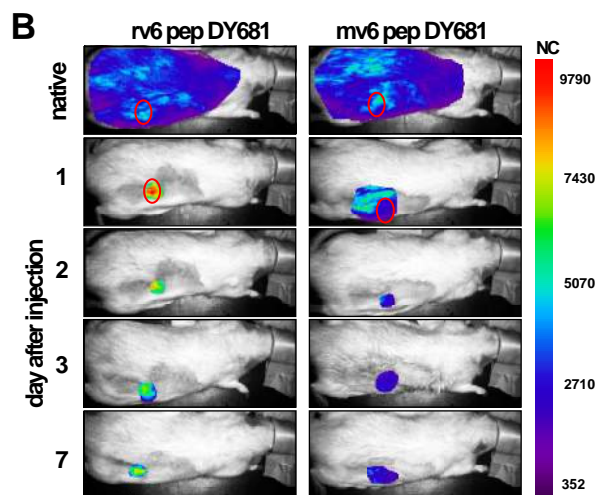
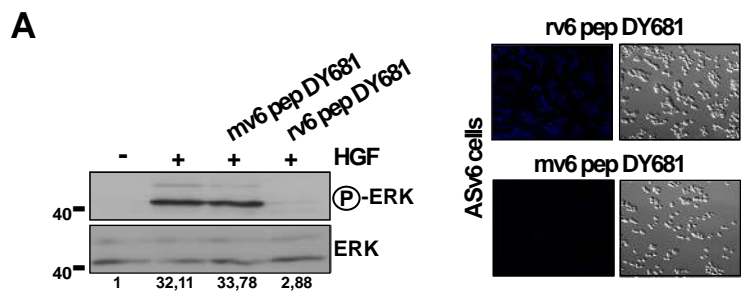
B Proliferation assay of Panc1 cells in absence and presence of HGF (20 ng/ml) and after preincubation with hv6pep (500 ng/ml). After 72 hours cells were counted using a brightfield microscope. The cell numbers were compared to the seeded cell number. Samples were measured in triplicates.

C HGF-induced migration and invasion of Panc1 cells using a transwell assay. Cells were treated with hv6pep or control peptide prior to induction with HGF 50 ng/ml in a Boyden chamber assay. After 24 hours cells were harvested from the bottom side of the filter and stained with crystal violet.

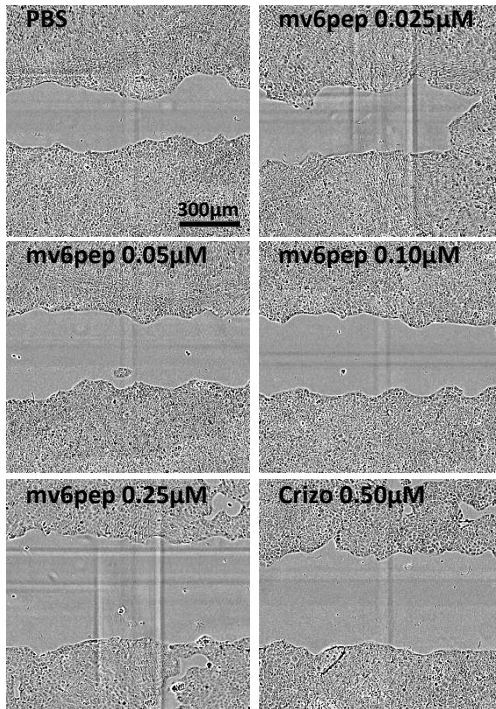
D Pictures of the tumor and pancreas after treatment with hv6pep respectively control peptide (top). Average tumor volume after three weeks of treatment (bottom).

Fig. S7 Serum stability of hv6pep (KEQWFGNRWHEGYR, A) and EQWFGNRWHEGY (B). Samples from a 500 μ M solution of either one of the peptides in human serum at 37 °C were taken at the indicated times, precipitated with the twofold volume of acetonitrile and 7 μ L of the supernatant analyzed by HPLC. The major metabolites in A were identified by LCMS as KEQWFGNRWHEGY (#) and EQWFGNRWHE (*).

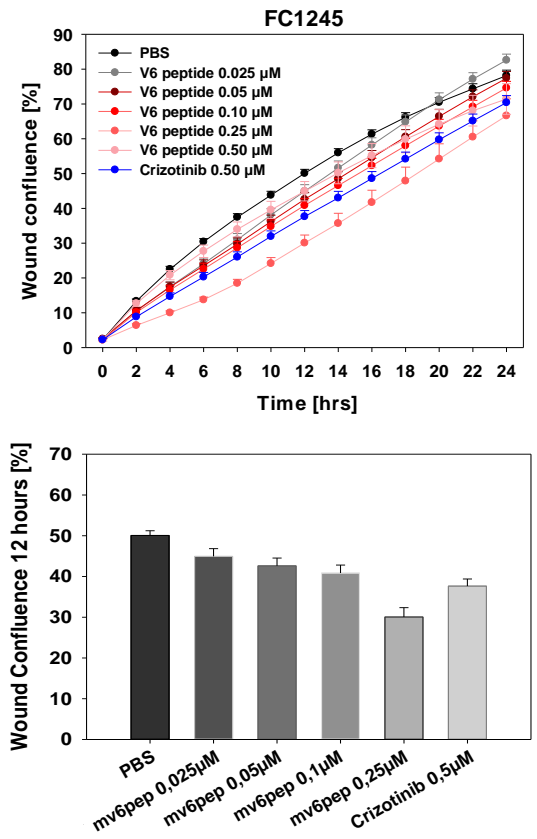




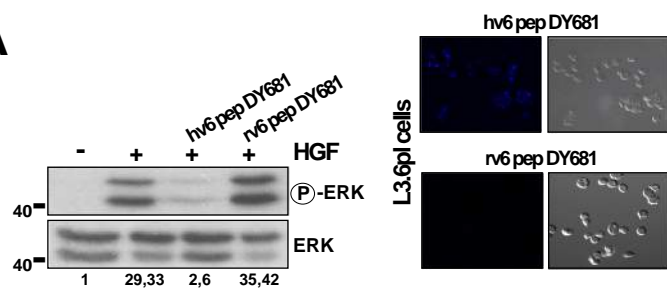
A



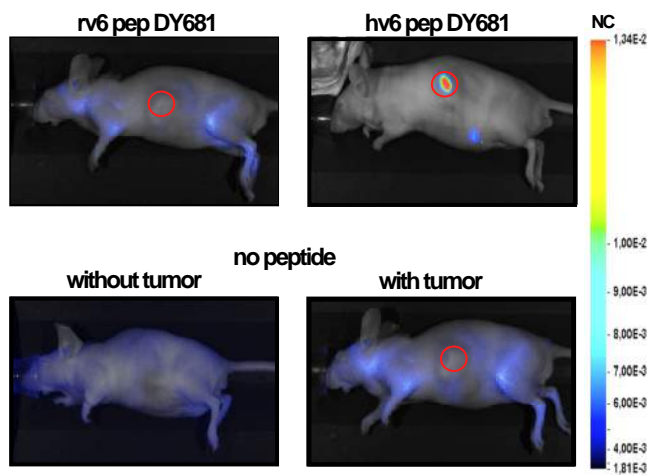
B



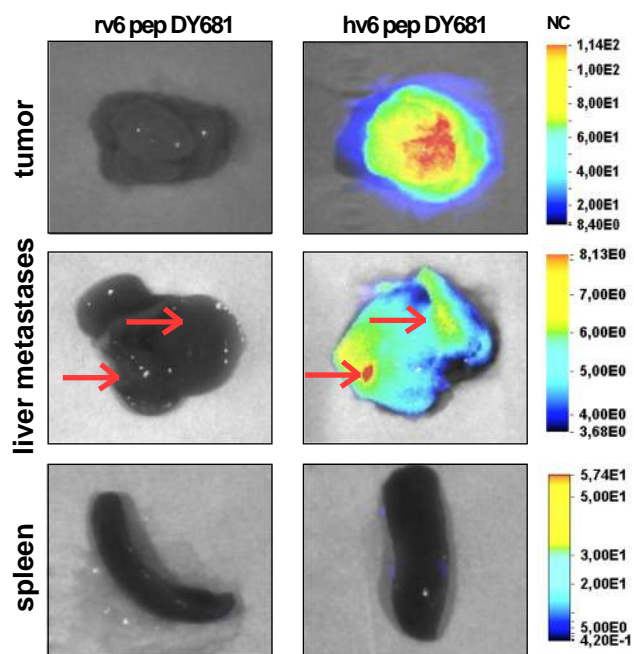
A



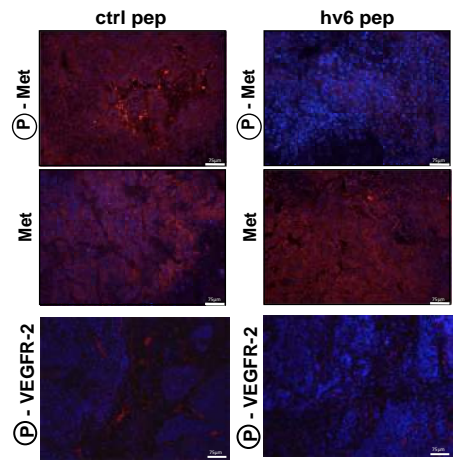
B



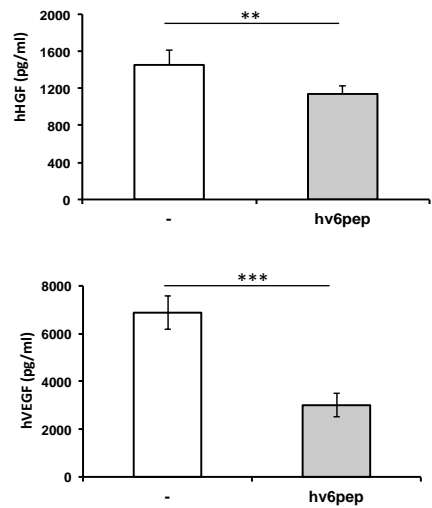
C



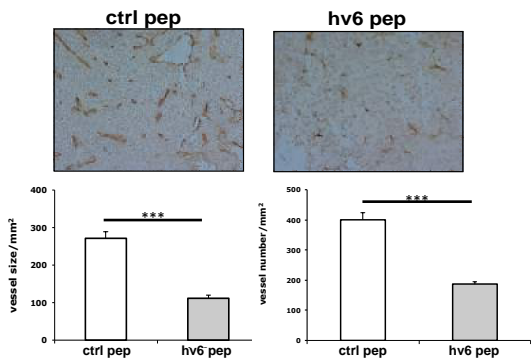
A

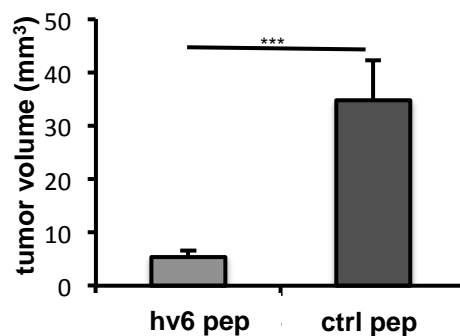
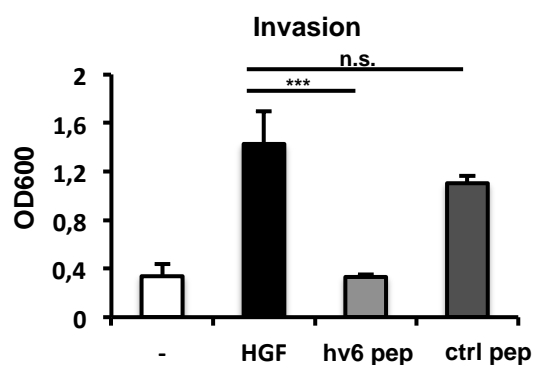
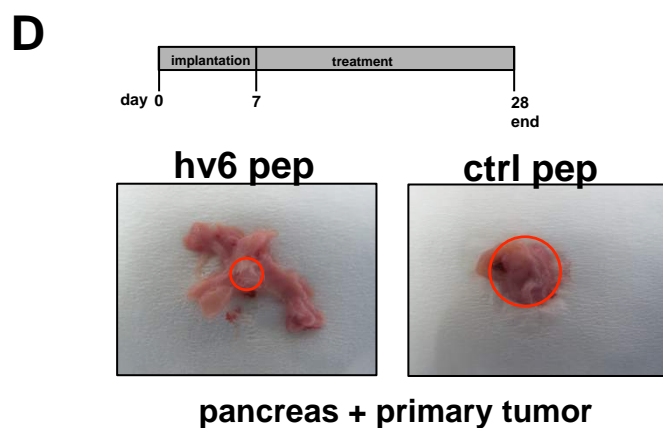
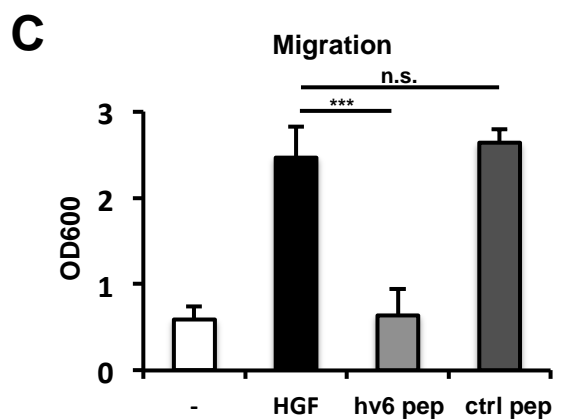
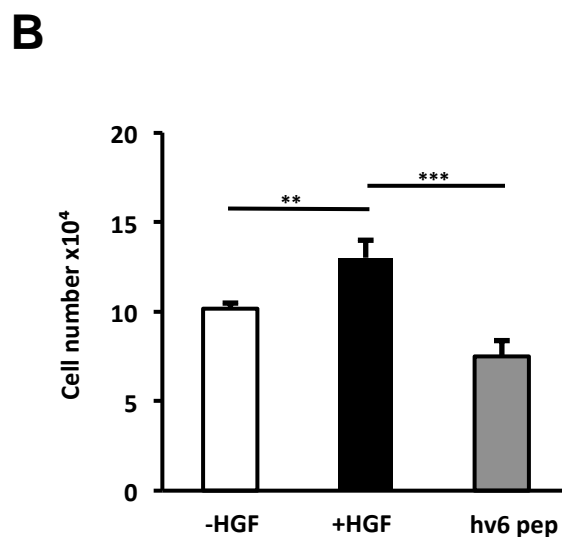
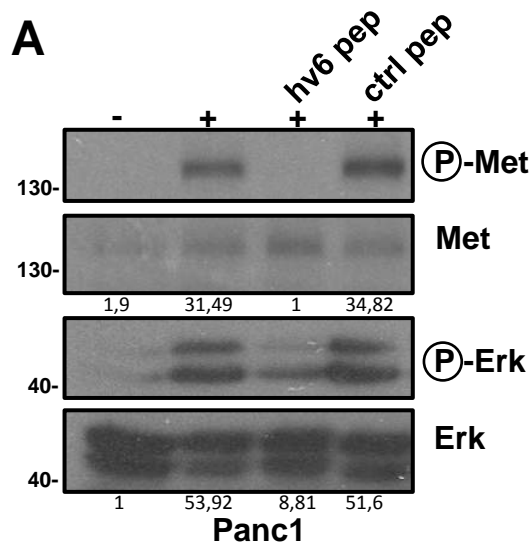


B

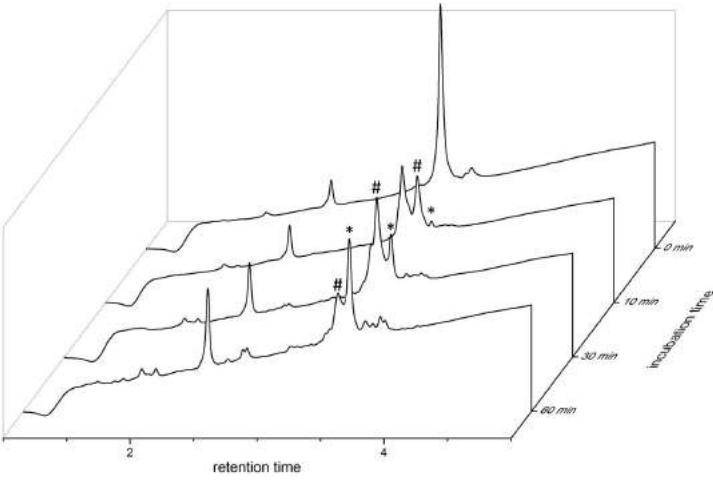


C





A



B

